European Journal of Medicinal Chemistry Reports 5 (2022) 100046

HOSTED BY

Contents lists available at ScienceDirect

European Journal of Medicinal Chemistry Reports

journal homepage: www.editorialmanager.com/ejmcr/default.aspx

Thiazolidin-4-one-based compounds interfere with the eicosanoid biosynthesis pathways by mPGES-1/sEH/5-LO multi-target inhibition

Ester Colarusso [a,1], Marianna Potenza [a,b,1], Gianluigi Lauro [a], Maria Giovanna Chini [c], Valentina Sepe [d], Angela Zampella [d], Katrin Fischer [b], Robert K. Hofstetter [b], Oliver Werz [b], Giuseppe Bifulco [a,*]

[a] Department of Pharmacy, University of Salerno, Via Giovanni Paolo II 132, Fisciano, 84084, Italy
[b] Department of Pharmaceutical/Medicinal Chemistry, Institute of Pharmacy, Friedrich Schiller University Jena, Philosophenweg 14, Jena, 07743, Germany
[c] Department of Biosciences and Territory, University of Molise, Contrada Fonte Lappone, Pesche, Isernia, I-86090, Italy
[d] Department of Pharmacy, University of Napoli, Via D. Montesano 49, Napoli, 80131, Italy

ARTICLE INFO

Keywords:
Thiazolidin-4-one
Virtual screening
Drug-repurposing
Inflammation
mPGES-1
sEH

ABSTRACT

Here we report the application of a multi-disciplinary protocol for investigating thiazolidin-4-one-based compounds as new promising anti-inflammatory agents interfering with the eicosanoid biosynthesis pathways. The workflow foresaw the generation of a focused virtual library of ~4.2×10^4 molecules featuring the thiazolidin-4-one core based on the related one-pot synthetical combinatorial route. The built library was initially screened *in silico* against the microsomal prostaglandin E_2 synthase-1 (mPGES-1) enzyme and, afterwards, 23 selected chemical items were synthesized for the subsequent biological screening, applying the one-pot multicomponent synthetic strategy. Preliminary results highlighted the moderate ability of several tested thiazolidin-4-one-based compounds in inhibiting mPGES-1. On the other hand, further computational repurposing investigations were performed on a set of synthesized compounds, highlighting the promising binding of a several items against the soluble epoxide hydrolase (sEH) enzyme, whose inhibition leads to an increase of epoxyeicosatrienoic acids (EETs) that are anti-inflammatory mediators. Three molecules (**3**, **9** and **21**) were able to inhibit sEH featuring IC_{50} values in the low micromolar range. In order to further profile their anti-inflammatory properties, additional investigations of the three identified hits highlighted their ability to inhibit 5-lipoxygenase (5-LO) and thus to interfere with leukotriene biosynthesis in neutrophils, devoid of activity against cyclooxygenases (COXs) and cytotoxic effects on human monocytes. Our results, obtained by applying a multidisciplinary approach, highlight the thiazolidin-4-one-core as a valuable template for developing novel anti-inflammatory compounds able to synergistically inhibit different targets involved in the arachidonic acid cascade.

1. Introduction

Prostaglandins E_2 (PGE_2) represent key effectors of inflammation, accomplishing a number of physiological functions while also being involved in different pathologic conditions, such as cell apoptosis, proliferation, angiogenesis as well as inflammation and immune surveillance [1]. PGE_2 are formed from free arachidonic acid (AA) by cyclooxygenases (COXs) in concert with specific terminal PG synthases (PGES, namely mPGES-1, mPGES-2 and cPGES) [2].

Differently from mPGES-2 and cPGES as constitutively expressed isoforms, mPGES-1 represents the inducible membrane-bound isoform, and it is involved in several acute and chronic disorders [3]. Accordingly, mPGES-1 inhibition aids the development of new promising and safer drugs blocking the inflammation-induced biosynthesis of PGE_2 [4] and, as a consequence, it represents a promising option in the treatment of chronic inflammation-related disorders. To date, different mPGES-1 inhibitors have been disclosed, and only two inhibitors entered clinical development phases, specifically GRC27864 (Glenmark Pharmaceuticals Ltd) and LY3023703 (developed by Eli Lilly). Importantly, LY3023703 approval process was interrupted due to its liver toxicity [3].

On the other hand, the fundamental role of soluble epoxide hydrolase (sEH) and epoxyeicosatrienoic acids (EETs) in inflammation and pain has

* Corresponding author.
E-mail address: bifulco@unisa.it (G. Bifulco).
[1] These authors contributed equally to this work.

https://doi.org/10.1016/j.ejmcr.2022.100046
Received 7 March 2022; Accepted 4 April 2022
Available online 12 April 2022

been broadly investigated in the last years. Soluble epoxide hydrolase (sEH) is responsible for EETs degradation to the corresponding dihydroxyeicosatrienoic acids (DHETs or DiHETrEs), leading to the lack of their biological benefits [5]. Moreover, several studies [5,6] have shown that sEH inhibitors decrease plasma levels of pro-inflammatory cytokines and nitric oxide metabolites, thus promoting the formation of lipoxins and supporting the resolution of inflammation.

Last, 5-LO catalyzes the first two steps of LTA_4 biosynthesis, which is involved in several inflammatory and allergic diseases, and several types of cancers [7]. Therefore, it is not surprising that the regulation of 5-LO activity has been the focal point of many therapeutic approaches in recent years.

During the last decade, we identified a number of mPGES-1 inhibitors featuring different chemical scaffolds [8–12]. With the aim of further exploring the chemical space, we have here investigated the thiazolidin-4-one scaffold for identifying anti-inflammatory/anticancer agents able to interfere with the above-reported inflammation-related targets, discovering the first mPGES-1/sEH/5-LO multitarget inhibitor.

The "privileged scaffold" feature of the thiazolidin-4-one has been widely analyzed in different studies, highlighting it as a template for developing agents able to play a key role in important diseases, such as acute inflammation and bacterial infections [13,14]. On the other hand, the thiazolidinone chemical platform is chemically related to the thiazolidine core, especially for what concerns the specific substitution patterns on the central ring showing a key role for establishing the interaction network with the protein counterparts. In this context, we recently reported [11] the related 2,4-thiazolidinedione core as an interesting scaffold for developing dual inhibitors of mPGES-1/5-LO, following also in this case a well-structured computational/experimental combined approach. Finally, the thiazolidin-4-one represents an unprecedented scaffold in the field of mPGES-1 inhibitors.

In light of all the considerations above, the thiazolidin-4-one was analyzed as a candidate for discovering novel anti-inflammatory agents targeting different enzymes in the arachidonic acid cascade by applying a well-structured workflow, involving computational investigations, chemical synthesis, and biological evaluation of the most promising hit compounds.

2. Results and Discussion

The workflow aimed at the identification of thiazolidin-4-one-based compounds as multi-target anti-inflammatory agents is depicted in Fig. 1. In the following paragraphs, detailed information regarding the different related steps is reported.

2.1. Building of the library of thiazolidin-4-one-based compounds and virtual screening on mPGES-1

In the frame of our research aimed at the identification of new anti-inflammatory agents targeting mPGES-1 [8–12], we firstly investigated the putative ability of thiazolidin-4-one-based compounds of inhibiting this enzyme through molecular modelling experiments. In this scenario, the availability of various high-resolution X-ray structures of human mPGES-1 co-complexed with different inhibitors (e.g. PDB code: 4BPM, 4AL1, 5BQG, 5BQH, and 5BQI) [15–17] represented a valuable source of information, especially for performing structure-based molecular docking experiments.

In more detail, the first step of the workflow here presented envisaged the generation of a virtual library of thiazolidin-4-one-based compounds following the related one-pot chemical synthesis procedure, leading to the possibility of differently decorating the central core by using aromatic aldehydes and substituted-2-amino-1-phenylethanones (*vide infra*). Specifically, the combination of ~3000 commercially available aromatic aldehydes and seven substituted-2-amino-1-phenylethanones, while also accounting the C-2 stereocenter leading to the formation of both the possible stereoisomers, allowed the generation of a library of $\sim 4.2 \times 10^4$ molecules (CombiGlide software, see Materials and methods) (Fig. 1).

Afterwards, the built library was tested by molecular docking experiments against mPGES-1 (PDB code: 4BPM), and the most promising compounds were filtered after carefully evaluating the docking score

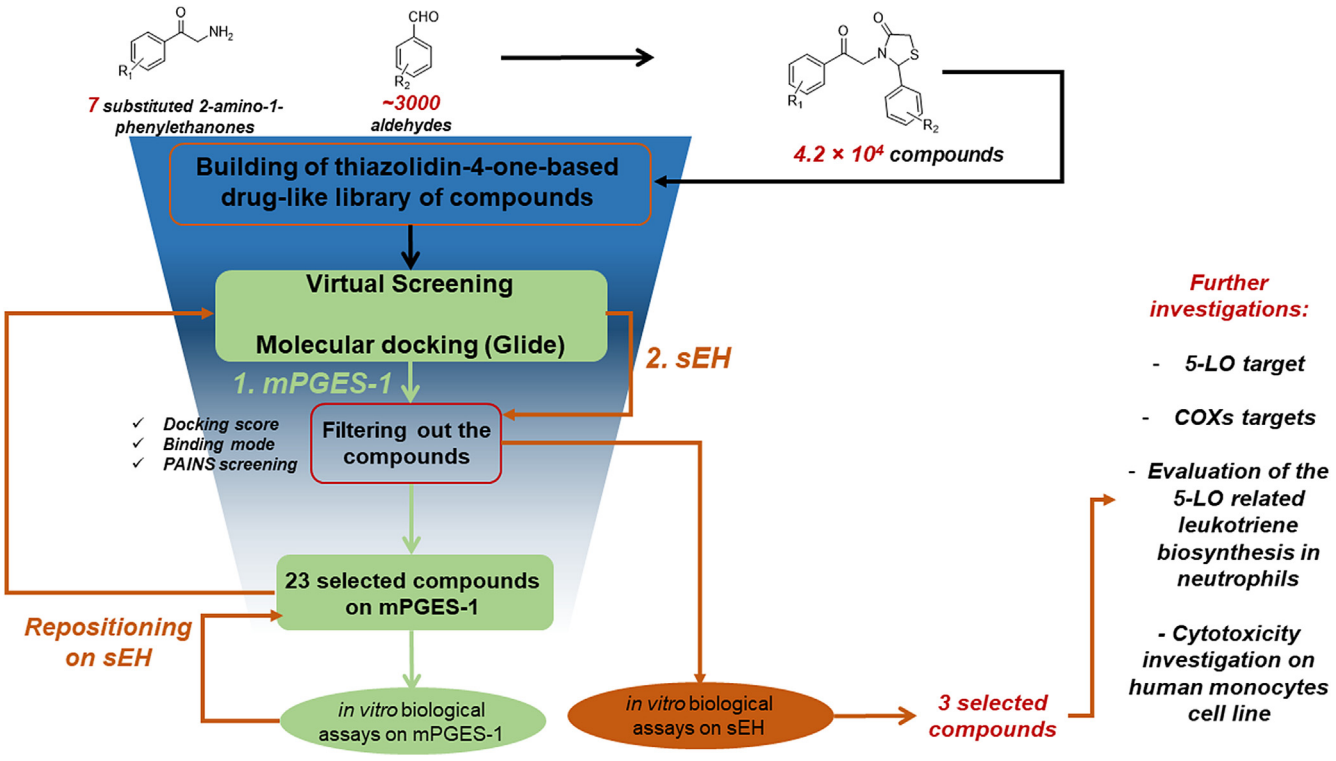

Fig. 1. The workflow for the selection of the thiazolidin-4-one-compounds. **(2-column fitting image, color should be used for figure in print)**.

values and analyzing the related binding modes. Specifically, the Virtual Screening Workflow implemented in Schrödinger Suite was employed, accounting the different HTVS, SP, and XP precision modes in Glide (see Materials and methods). In this way, the first ~1000 compounds were roughly filtered out accounting −6.0 kcal/mol as XP score cutoff. Afterwards, these items were further selected, carefully analyzing their binding mode and the interaction pattern with the receptor counterpart.

mPGES-1 is a glutathione (GSH)-dependent membrane protein structurally organized as a homotrimer, thus showing three equivalent monomers or chains (here named A, B, and C) (Fig. 2A). mPGES-1 features three equivalent active sites within the membrane-spanning region, each of them with one GSH cofactor molecule and characterized by different residues belonging to the two adjacent monomers. Due to the different chemical features of the residues and their three-dimensional arrangement, different regions in the mPGES-1 binding site can be identified (Fig. 2B). Firstly, a groove is evident between the GSH binding site and a molecular region close the cytoplasmic part of the protein, with both aromatic (B:Phe44, B:His53) and polar (B:Asp49) residues (Fig. 2B). GSH as cofactor is located in a deep cavity and, due to the strong interactions between its two terminal carboxylate functions and the positively charged residues of mPGES-1 (B:Arg38, A:Arg73), it features a characteristic U-shape conformation (Fig. 2B). Moving to the cytoplasmic part of the protein, a binding groove is between helix 1 of chain B and helix 4 of chain A, comprising polar (A:Gln134), aliphatic (B:Val24) and aromatic (A:Tyr130, B:Tyr28) residues (Fig. 2B).

Starting from these structural information, the most promising compounds were visually inspected (Fig. 2C–D) and selected accounting the following interaction pattern:

- interactions with B:Phe44 and/or B:His53 (H–bonds, hydrophobic, face-to-face and/or edge-to-face π-π interactions);
- polar contacts with A:Arg126, A:Thr131, B:Gln36, B:Asp49;
- interactions with GSH and with A:Tyr130, a key residue interacting with GSH as cofactor.

In general, the careful analysis of the docking poses disclosed the partial ability of the thiazolidin-4-one-based compounds to establish the above-reported interactions with the receptor counterpart and a quite different binding mode if compared with that of compounds featuring the 2,4-thiazolidinedione previously reported by us [11]. Starting from a first set of filtered items, and in order to define a minimal structure-activity relationship (SAR), a subset of compounds was further selected with the aim of investigating the influence of both electron withdrawing/electron donor substituents on the aromatic ring of the phenyl-2-oxoethyl moiety at N-3 while maintaining a focused group of aldehydes derived substituents at C-2. Following this scheme, 23 compounds (**1**–**23**) were filtered (Fig. 3) and, prior to the chemical synthesis phase, the selected items were further screened for the "Pain Assay Interference compounds" (PAINS) identification, employing SwissADME software [18]. None of the selected compounds were classified as PAINS after this screening. Also, analyzing the binding modes of all the most promising compounds **1**–**23**, we did not detect a systematic selection of poses related to a specific stereoisomer able to satisfy the above-reported selection filters. Accordingly, we speculated that, apart the chemical differences arising from the specific substituents on the central core leading to the different selected compounds, the absolute configuration at C-2 did not represent a key structural point for systematically assuring

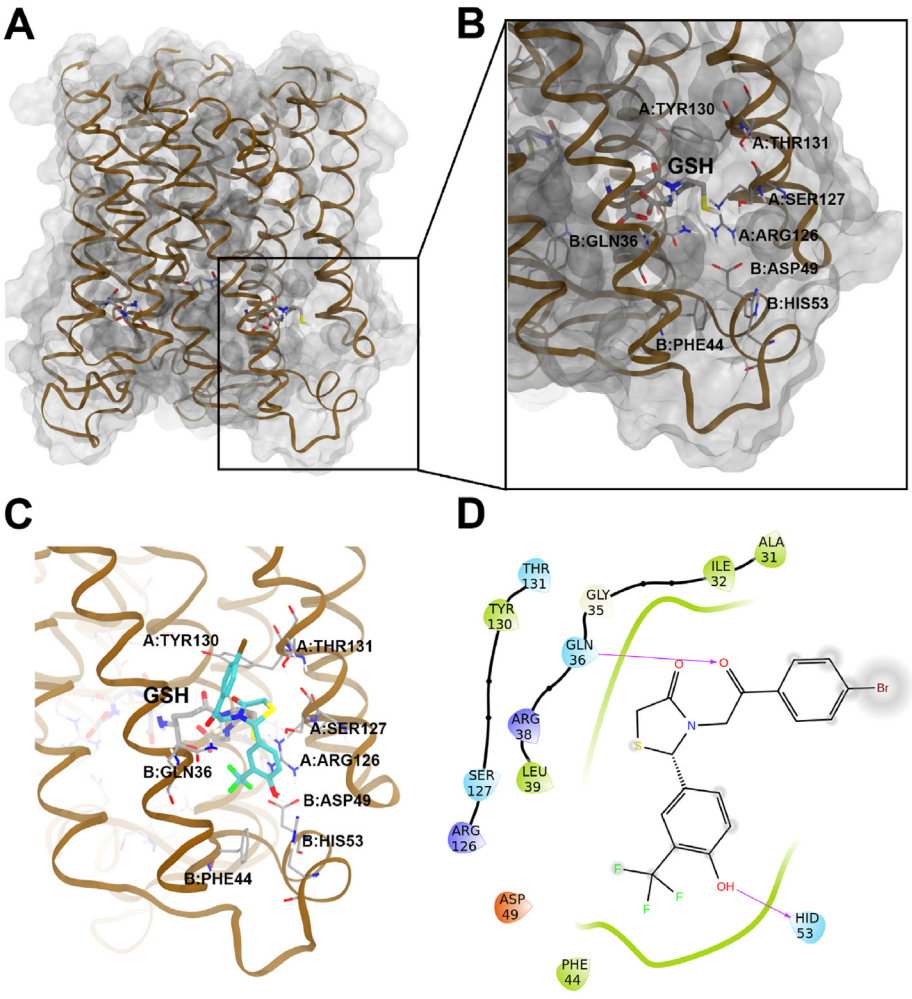

Fig. 2. a) Molecular representation of the mPGES-1 trimer (secondary structure reported in brown ribbons, molecular surface represented in transparent grey); b) mPGES-1 binding site; glutathione (GSH) cofactor and the key-residues in the mPGES-1 binding site are represented in sticks (C, grey; O, red; N, blue; polar H light grey); c) selected 3D pose of **9** (see Fig. 3) (colored by atom types: C, cyan; N, blue; O, red; S, yellow; polar H, light grey; F, light green; Br, brown) in docking with mPGES-1 (secondary structure focused to the mPGES-1 binding site colored in brown; glutathione (GSH) cofactor and key-residues in the mPGES-1 binding site are represented in sticks colored by atom types: C, grey; O, red; N, blue; S, yellow; H light grey); d) related two-dimensional panels representing interactions (violet arrows representing H-bonds). Neutral histidine with hydrogen on the δ nitrogen is reported as HID. **(2-column fitting image, color should be used for figure in print)**.

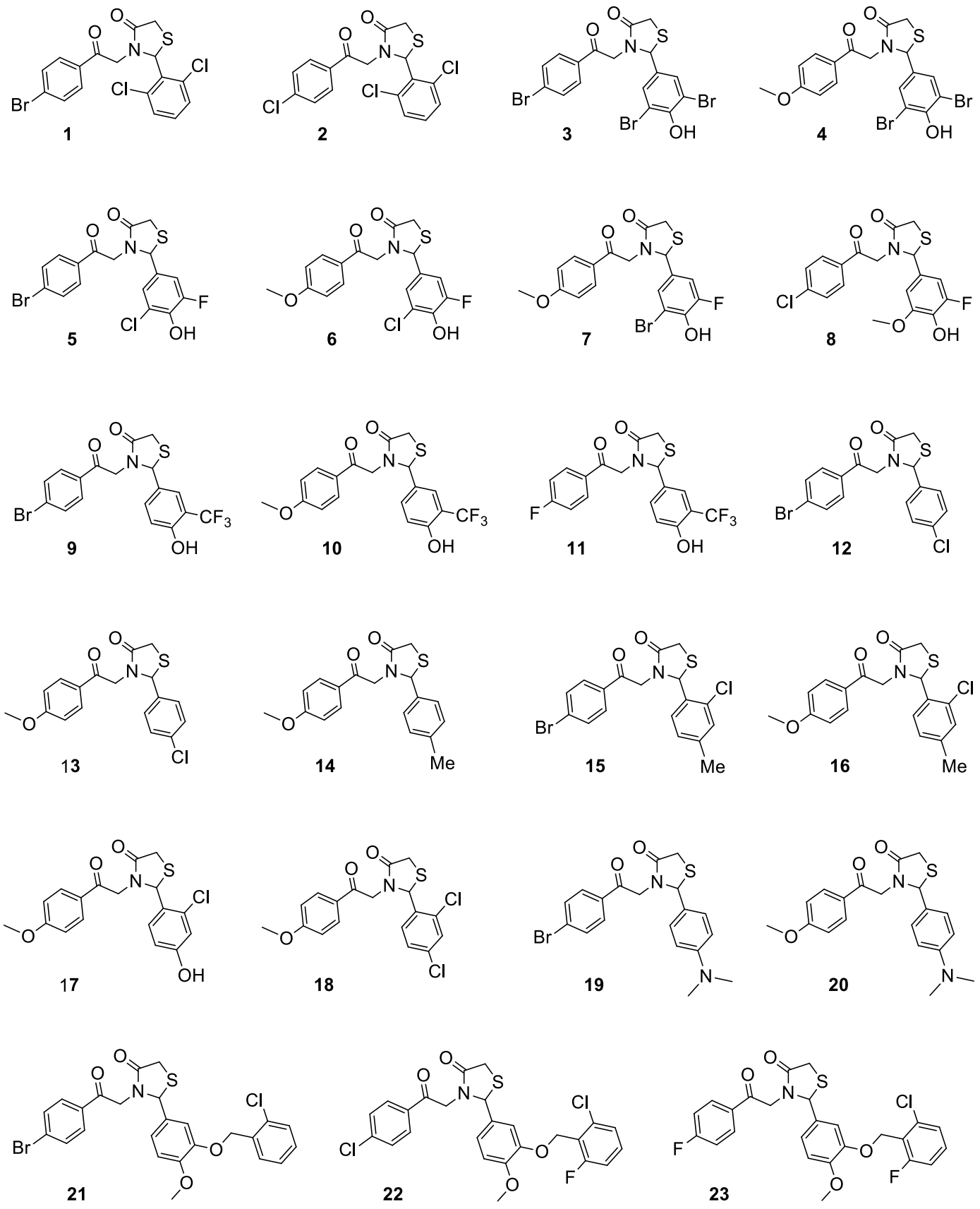

Fig. 3. Selected and synthesized thiazolidin-4-one-based molecules **1-23**. **(2-column fitting image)**.

the respect of the interaction patterns with the residues belonging to mPGES-1. Afterwards, for each selected compound, we retrospectively and carefully evaluated the binding modes of both the possible stereoisomers, confirming this behavior. Specifically, the two different enantiomeric species show different binding modes, as expected, but, on the other hand, the respect of the key interactions with the protein counterpart was observed for both the possible isomers, thus indicating that they can in principle feature a promising binding mode with the protein counterpart (see Fig. S1, Supporting Information).

2.2. Chemistry

The strategy for the synthesis of the identified molecules is shown in Scheme 1. The reaction was performed between substituted-2-amino-1-phenylethanone hydrochloride, an aromatic aldehyde, and an excess of mercaptoacetic acid in dry toluene under reflux. The choice was oriented towards a one-pot multicomponent reaction, considering the possibility of easily integrating it with the above-reported computational combinatorial approach. Accordingly, a large number of molecules deriving from the virtual screening outcomes may be quickly synthesized. Also, the application of "green" approaches in medicinal chemistry is nowadays preferred to the traditional synthetic methods [19], and one-pot chemical routes (Scheme 1) are even more accounted with this aim, considering the limited number of synthetic steps and the reduction in the amount of reagents and solvents needed. In detail, we started from a two-step strategy [20], which proceeds with the imine formation followed by cyclization with the addition of mercaptoacetic acid under mild conditions. Additionally, one-pot methods have already been reported, but catalysts [21], bases [22] supports [23] or microwave [24] are needed for these strategies. In our case, the reaction proceeded with good yields in relatively fast reaction times (see Materials and methods) without the addition of bases or catalysts. Interestingly, the 23 compounds were synthesized with different yields (from 45% up to 95%) according to the specific benzaldehyde and the 2-amino-1-phenylethanone adopted for the reaction. Benzaldehydes bearing only electron donor groups on the aromatic ring (compounds **14**, **19**, **20**), gave the lowest yields according to the low reactivity of the carbonyl group, while the best yields were obtained in the reactions in which the benzaldehyde partner was more reactive (compounds **1**, **2**, **18**) due to the presence of electron-withdrawing groups. Comparing compounds with the same benzaldehyde, a slight improvement in the yield of the reaction was detected when 2-amino-1-phenylethanone was more basic, due to the presence of an electron donor group.

2.3. In vitro evaluation of the inhibitory activity of compounds 1–23 on mPGES-1

A cell-free assay [25] (see Materials and methods) was performed for the screening of compounds **1–23** against microsomal prostaglandin E_2 synthase-1 (mPGES-1), thus preliminarily investigating the putative inhibitory activity of **1**–**23**. Specifically, all the compounds were tested at a concentration of 10 μM, and nine among them reduced the enzyme activity, spanning from ~25 to ~50% inhibition (**1**, **3**, **5**, **7**, **9**, **11**, **17**, **18**, **21**). At the same time, a slight inhibitory potency was found in the remaining compounds (see Table 1). Thus, compounds **1–23** disclosed only a partial inhibition of the activity of mPGES-1. In particular, this behavior was ascribed to the moderate ability of the non-aromatic chemical core of thiazolidin-4-one establishing all the set of interactions with the key residues in the receptor counterpart as well as to correctly orient the substituents at C-2 and N-3 in the binding pocket. In Fig. 2C, the binding mode of compound **9** that, together with **11**, was most efficient against mPGES-1 (reduction of mPGES-1 activity = ~50% at 10 μM), is depicted.

Table 1
Values of the residual activity of microsomal prostaglandin E_2 synthase-1 (mPGES-1) after incubation with compounds **1**–**23**, and residual activity of human soluble epoxide hydrolase (sEH) after incubation with compounds **3**, **5**, **6**, **8**–**11**, **19**, **21**–**23** at a concentration of 10 μM. Data are expressed as percentage of control (100%), $n = 3$. MK-886 (10 μM) and AUDA (5 μM) were used as reference compounds for mPGES-1 and sEH cell-free assays, respectively.

Compound	Residual activity of mPGES-1 (%) ± SD	Residual activity of sEH (%) ± SD
1	65.2 ± 2.0	nt[a]
2	76.5 ± 1.6	nt[a]
3	65.9 ± 1.1	37.8 ± 1.1
4	84.4 ± 1.5	nt[a]
5	72.1 ± 0.5	57.0 ± 1.3
6	84.9 ± 1.5	100.4 ± 1.0
7	63.3 ± 1.8	nt[a]
8	90.6 ± 2.6	80.0 ± 0.8
9	55.6 ± 1.6	36.9 ± 1.0
10	85.3 ± 2.2	94.1 ± 1.5
11	48.0 ± 1.0	65.9 ± 1.0
12	88.9 ± 0.8	nt[a]
13	88.4 ± 3.1	nt[a]
14	84.9 ± 0.5	nt[a]
15	79.3 ± 1.4	nt[a]
16	79.5 ± 1.1	nt[a]
17	72.6 ± 2.0	nt[a]
18	74.6 ± 0.9	nt[a]
19	87.1 ± 1.5	59.3 ± 0.9
20	77.8 ± 0.6	nt[a]
21	72.7 ± 1.8	40.3 ± 1.2
22	84.0 ± 2.3	75.0 ± 1.3
23	88.2 ± 1.3	84.1 ± 1.5
MK-886	25.3 ± 1.1	nt[a]
AUDA	nt[a]	15.0 ± 0.9

[a] nt: not tested.

2.4. Repurposing, virtual screening, and biological evaluation of the synthesized subset of thiazolidin-4-one-based compounds on soluble epoxide hydrolase (sEH)

Starting from the partial inhibitory activities obtained for compounds **1–23** against mPGES-1, we wondered whether these chemical entities could interfere with further biological targets involved in formation of inflammation-related lipid mediators. Specifically, we performed a computational investigation against the soluble epoxide hydrolase (sEH) target by means of molecular docking calculations. This choice was made since the sEH inhibitor chemotype is typically endowed with 1,3-aromatic disubstituted urea function, thus sharing a similar shape and substitution pattern with the investigated thiazolidin-4-one-based compounds [26]. In addition, we assumed that the hydrophobic groups at position 2 and 3 on the thiazolidin-4-one ring may be a key feature for the inhibition, considering the hydrophobic profile of the sEH active site,

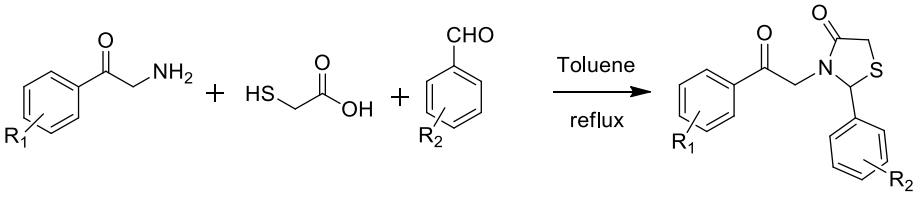

Scheme 1. Synthetic strategy adopted for the synthesis of compounds **1–23**. **(1-column fitting image)**.

enforcing this repositioning study [27]. Moreover, the importance of this target is relevant in the treatment of inflammatory disorders [28], and several studies [26,29] were focused on the identification of promising inhibitors of sEH, with three candidates that entered clinical trials [30–32].

sEH shows two catalytic domains: the domain for the lipid epoxide hydrolase activity (sEH-H) is in the C-terminal half, while the phosphatase activity (sEH-P) is located in the N-terminal domain [33]. The role of sEH-H in the hydrolysis of epoxides of polyunsaturated fatty acids was widely investigated, while the role of sEH-P is still unclear [33]. The widely investigated chemical mechanism of the enzyme related to the hydrolase activity is mainly based on a catalytic triad (Asp335, His524, Asp496). Specifically, the epoxide group of the substrate is firstly polarized by two tyrosine residues (Tyr383 and Tyr466), while Asp335, which is in turn activated and oriented towards His524 and Asp496, performs the nucleophilic attack with its carboxylic group [34].

Starting from the reported structural considerations, we performed a focused Virtual Screening accounting for the small library of synthesized compounds **1**–**23** against sEH. The evaluation of the predicted docking scores and the careful analysis of the interactions between the docking poses and the receptor counterpart led to the further selection of ten compounds (**3**, **5**, **6**, **8**–**11**, **19**, **21**–**23**) to be submitted to subsequent biological evaluation. The analysis of the docking poses highlighted the substituents at N-3 being accommodated onto the deeper part of the binding site and close to the residues involved in the catalytic mechanism. We speculated that electron-withdrawing substituents on the phenyl-2-oxoethyl moiety at N-3 could be useful for gaining interactions with the Asp335 residue and, to corroborate this hypothesis, two negative controls (**6** and **10**, featuring the 4-methoxy-phenyl-2-oxoethyl substituents at N-3) were also selected.

Afterwards, a cell-free assay (see Materials and methods section) [35] was applied for screening the selected compounds **3**, **5**, **6**, **8**–**11**, **19**, **21**–**23** against human soluble epoxide hydrolase (sEH), in order to corroborate the computational predictions. The compounds were tested at a concentration of 10 μM. Interestingly, among the compounds bearing a benzyloxy moiety in *meta* position on the phenyl ring at C-2 of the thiazolidinone (**21**, **22** and **23**), only **21**, bearing a bromine atom, inhibited the activity of the enzyme by more than 50% (Table 1). Considering the other set of compounds (**3**, **5**, **6**, **8**–**11**, **19**), inhibition of the activity by >40% in comparison to the control (100%) was observed for **3**, **5**, and **9** (Table 1), all of them keeping the 4-Br-phenyl-2-oxoethyl moiety at N-3 as in compound **21**, and variously substituted *p*-hydroxy phenyl rings at C-2. Also, reduction of the activity by 35% was observed by replacing the bromine with a fluorine atom (compound **11**). Compound **19**, featuring the 4-Br-phenyl-2-oxoethyl moiety at N-3, while showing a *N*,*N*-dimethyl substituent in *para* on the phenyl ring at C-2, inhibited sEH activity by 40%. Interestingly, compounds **6** and **10**, both bearing a donor group (a methoxyl group) in *para* on the phenyl-2-oxoethyl moiety at N-3, did not show inhibitory potency against the enzyme, thus confirming our hypothesis. A concentration-response analysis was conducted for compounds that at 10 μM inhibited the activity of the enzyme by >50% (Fig. S51, Supporting Information). The enzyme was incubated with compounds **3**, **9**, and **21** at concentrations from 0.3 up to 30 μM, and the related IC_{50} values were calculated (Table 2), disclosing their inhibitory activities against human sEH in the low micromolar range.

In Fig. 4A–F the binding modes and the interactions between compounds **3**, **9**, and **21** as the most promising inhibitors and sEH are reported, highlighting the key role of the 4-Br-phenyl-2-oxoethyl at N-3 able to interact with the key residues involved in the catalytic chemical mechanism of the enzyme and, in particular, with Asp335 bearing the negatively charged carboxylate function in the side chain.

Table 2
Residual activity and IC_{50} values of compounds **3**, **9**, and **21** against isolated enzymes involved in the formation of inflammation-related lipid mediators. Data of the residual enzyme activity at 10 μM test compound concentration are expressed as percentage of vehicle control (100%) and are given as means ± S.E.M. for n = 4. Zileuton (3 μM) and Indomethacin (10 μM) were used as reference compounds for 5-LO and COXs assays, respectively.

Compound	IC_{50} ± S.E.M. for sEH (μM)	5-LO residual activity (%)	IC_{50} ± S.E.M. for 5-LO (μM)	COX-1 residual activity (%)	COX-2 residual activity (%)
3	6.3 ± 0.4	60.7 ± 0.9	nt[a]	n.i.[a] (>90)	n.i.[a] (>90)
9	6.1 ± 0.3	17.6 ± 1.1	5.0 ± 0.7	n.i.[a] (>90)	n.i.[a] (>90)
21	6.2 ± 0.6	70.1 ± 1.7	nt[a]	n.i.[a] (>90)	n.i.[a] (>80)
Zileuton	nt[a]	34.0 ± 2.1	nt[a]	nt[a]	nt[a]
Indomethacin	nt[a]	nt[a]	nt[a]	25.1 ± 1.0	34.5 ± 0.6

[a] nt: not tested; n.i.: not inhibition.

2.5. Biological screening of compounds *3, 9 and 21* against COXs and 5-LO

Considering the reported inhibition of the activity of COX and the selective inhibitory activity of COX-2, specifically for 4-thiazolidinone derivatives [36], we investigated the ability of compounds **3**, **9**, and **21** to inhibit the catalytic activities of COX isoenzymes. A cell-free assay [35] using isolated COX-1 and COX-2 enzymes was used for this analysis (see Materials and methods section). Interestingly, compounds **3**, **9**, and **21** did not exhibit significant inhibitory activity on COX-1 and -2. Next, the test compounds were evaluated in a cell-free 5-LO activity assay, in order to verify their ability to interfere with leukotrienes biosynthesis. Intriguingly, **3** and **21** (10 μM, each) inhibited 5-LO activity by 39% and 30%, respectively, whereas the strongest inhibitory effects were evident for compound **9**. Concentration-response analysis of **9** (from 0.1 up to 10 μM, Fig. S52, Supporting Information) disclosed an IC_{50} value in the low micromolar range (5.0 μM, Table 2).

2.6. Evaluation of the compounds for inhibition of leukotriene biosynthesis in neutrophils and for cytotoxic effects against human monocytes

Next, the capability of the test compounds **3**, **9**, and **21** for blocking 5-LO-mediated LT biosynthesis was investigated in intact neutrophils from human peripheral blood. The compounds were tested at 10 μM in two different experimental settings, using (i) Ca^{2+}-ionophore or (ii) Ca^{2+}-ionophore plus arachidonic acid to evoke LT formation. Interestingly, compounds **3** and **9** inhibited the formation of LTB_4 and its isomers as well as 5-H(p)ETE with IC_{50} values in the low micromolar range (21.8–4.4 μM, depending on the assay conditions, Fig. 5) whereas only a slight inhibition of 5-LO product formation was observed for compound **21** (Table 3). Thus, these results from the cell-based assay on human neutrophils showed a comparable efficiency profile of **3**, **9**, and **21** for inhibition of 5-LO/LT formation in intact cells and inhibition of isolated 5-LO (Table 3).

Finally, a cytotoxicity assay with human monocytes was performed in order to investigate possible detrimental effects of compounds **3**, **9**, and **21** on cell viability. Monocytes were treated with the test compounds (10 μM), Triton (1%, positive control) or vehicle (0.5% DMSO) for 24 h, and an MTT assay was performed. None of compounds **3**, **9**, and **21** reduced the viability of monocytes, whereas the positive control strongly reduced cell viability under the same conditions (Fig. S53, Supporting Information).

3. Conclusions

Here we reported an efficient multistep protocol, in which the computational design part was coupled to a one-pot multicomponent synthetic strategy, with the purpose of investigating the inhibitory potency of variously decorated thiazolidin-4-one derivatives against mPGES-1. Considering that a modest inhibitory activity of the thiazolidin-4-one-based compounds (**1**–**23**) on mPGES-1 was identified,

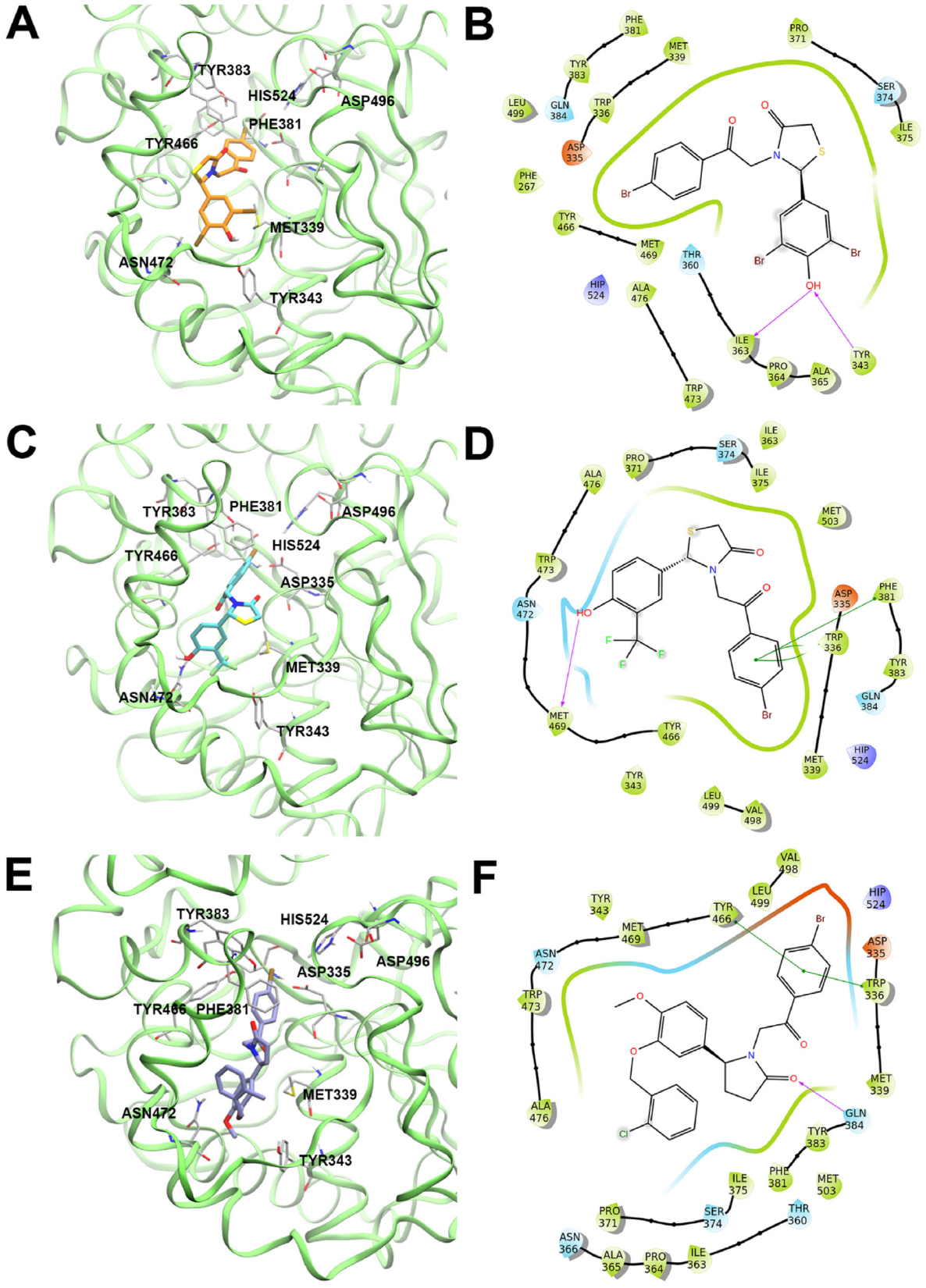

Fig. 4. Selected 3D poses and related two-dimensional panels representing interactions (violet arrows representing H-bonds, and green lines representing π-π stacking interactions) of a,b) **3** (colored by atom types: C, orange; N, blue; O, red; S, yellow; polar H, light grey; Br, brown); c,d) **9** (colored by atom types: C, cyan; N, blue; O, red; S, yellow; polar H, light grey; F, light green; Br, brown); e,f) **21** (colored by atom types: C, light violet; N, blue; O, red; S, yellow; polar H, light grey; Cl, green; Br, brown) in docking with soluble epoxide hydrolase (sEH) (secondary structure focused to the sEH binding site colored in green; key-residues are represented in sticks colored by atom types: C, grey; O, red; N, blue; S, yellow; H light grey). **(2-column fitting image, color should be used for figure in print)**.

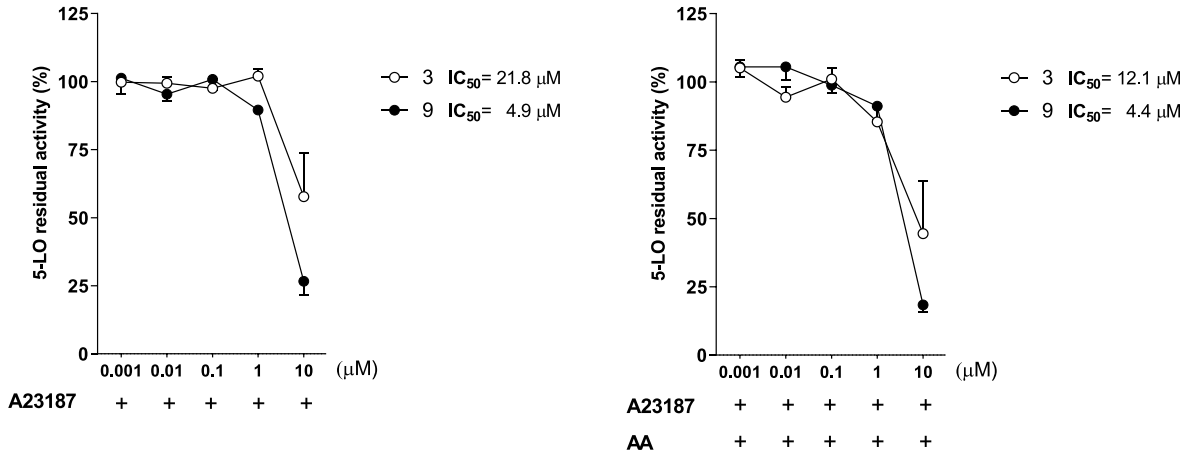

Fig. 5. Concentration-response analysis for inhibition of 5-LO product formation in intact human neutrophils. Cells were pre-incubated with compound **3**, **9** or vehicle (0.1% DMSO) for 10 min at 37 °C, and then stimulated with 2.5 μM Ca^{2+}-ionophore A23187 for another 10 min (left) or with 2.5 μM Ca^{2+}-ionophore A23187 plus 20 μM arachidonic acid for another 10 min (right). The incubations were terminated on ice and 5-LO products were analyzed by RP-HPLC. Data are expressed as percentage of vehicle control (100%), means ± S.E.M., $n = 3$ (compound **3**); $n = 4$ (compound **9**). **(1-column fitting image)**.

Table 3
5-LO product formation in intact neutrophils after incubation with compounds **3**, **9**, and **21**. Cells were stimulated either with A23187 or with A23187 plus AA. Data are expressed as percentage of vehicle control (100%) at test compound concentration of 10 μM (means ± S.E.M.) of $n = 6$; IC_{50} values of $n = 3$ (compound **3**); $n = 4$ (compound **9**). Zileuton (3 μM) was used as reference compound.

Compound	Residual 5-LO product formation (%) evoked with A23187	Residual 5-LO product formation (%) evoked with A23187 plus AA	IC_{50} value (μM) evoked with A23187	IC_{50} value (μM) evoked with A23187 plus AA
3	25.5 ± 6.9	64.2 ± 6.0	21.8 ± 7.4	12.1 ± 4.4
9	28.6 ± 7.0	19.9 ± 5.3	4.9 ± 0.6	4.4 ± 0.2
21	70.8 ± 12.7	53.2 ± 7.1	nt[a]	nt[a]
Zileuton	39.5 ± 3.1	46.3 ± 4.3	nt[a]	nt[a]

[a] nt: not tested.

the same class of compounds was subjected to a computational repurposing on the human soluble epoxide hydrolase (sEH), with the main purpose of investigating the inflammatory activity of thiazolidinone-based compounds exploring additional inflammation-related lipid mediator pathways. In particular, the focus was placed on sEH, due to the amide group belonging to the thiazolidin-4-one ring that is a typical pharmacophoric point of sEH inhibitors. Results from virtual screening experiments on sEH pointed towards ten items out of the 23 compounds and, after biological evaluation, **3**, **9**, and **21** showed indeed good inhibitory activity against sEH ($IC_{50} \sim 6$ μM), paving the way to further insights in the unexplored field of cyclic amide-based inhibitors. Cell-free assays on COXs and 5-LO with the hits **3**, **9**, and **21** expanded our investigations of interference with inflammation-related lipid mediator biosynthesis, revealing compound **9** as promising 5-LO inhibitor, with somewhat reduced potencies for compounds **3** and **21**. Finally, the capability of the test compounds for reducing 5-LO-mediated LT production in intact human neutrophils was confirmed by the efficient inhibition of 5-LO in the cellular context.

Together, these results represent a valuable starting point for an optimization campaign towards the identification of promising hits belonging to the novel class of thiazolidinone-based multiple modulators of lipid mediator-producing enzymes, paving the way to further investigation for accelerating the identification of multi-target inhibitors interfering with the eicosanoid biosynthesis. The multidisciplinary applied approach represented a powerful and useful tool in achieving the reported outcomes.

4. Materials and methods

4.1. Computational details

4.1.1. Building of a combinatorial library and virtual screening

Following the chemical route for the decoration of the investigated scaffold (Scheme 1), a virtual library of thiazolidin-4-one-based compounds was built using the Interactive Enumeration tool of the CombiGlide software [37] as input for the subsequent molecular docking calculations. For the decoration of the central core, the following starting reagents were considered after checking their commercial availability:

- aldehydes: 3013 items;
- 2-amino-1-phenylethanones, differently substituted on the phenyl ring: 7 items.

The starting core and all the reagents were then combined, also accounting the C-2 stereocenter thus leading to both the possible stereoisomers, for producing the final library of compounds ($\sim 4.2 \times 10^4$ molecules).

4.1.2. Virtual screening on mPGES-1

Protein 3D model was prepared using the Schrödinger Protein Preparation Wizard, [54] starting from the mPGES-1 X-ray structure in the active form co-complexed with the inhibitor LVJ (2-[[2,6-bis(chloranyl)-3-[(2,2-dimethylpropanoylamino)methyl]phenyl]amino]-1-methyl-6-(2-methyl-2-oxidanyl-propoxy)-N-[2,2,2-tris(fluoranyl)ethyl]benzimidazole-5-carboxamide) (PDB code: 4BPM). The careful analysis of this protein crystal structure revealed that the binding of the reference co-crystallized inhibitor (LVJ) was not assisted by water molecules, and, accordingly, they were removed for the subsequent molecular docking experiments. Afterwards, all hydrogens were added, and bond orders were assigned.

The Virtual Screening was performed using the Virtual Screening Workflow using Glide software [38], following the scheme:

- High-Throughput Virtual Screening Glide mode (HTVS) phase, 1 pose retained for each compound, saved first 20% of ranked compounds;
- Standard Precision Glide mode (SP) phase, 1 pose retained for each compound, saved first 20% of ranked compounds;
- Extra Precision Glide mode (XP) phase, saved 20 maximum number of poses for each compound, saved all the ranked compound poses as final output.

The filtered compounds were then ranked considering the XP Glide docking score. Afterwards, they were visually inspected and selected, evaluating the respect of the key interactions (Results and Discussion section) for the subsequent chemical synthesis phase.

4.1.3. Virtual screening on soluble epoxide hydrolase (sEH)

Protein 3D model was prepared using the Schrödinger Protein Preparation Wizard [38], starting from the sEH X-ray structure in the active form co-complexed with the inhibitor BSU (1,3-diphenylurea) (PDB code: 5AI5). The visual inspection of this protein crystal structure revealed that the binding of the co-crystallized inhibitor (BSU) was not assisted by water molecules and, for this reasons, we removed them for the subsequent molecular docking experiments. Then, all hydrogens were added and bond orders were assigned.

The molecular docking experiments on the 23 synthesized compounds (Fig. 3), previously built *in silico* (Virtual Screening on mPGES-1 section, Computational Details) were performed using Glide software, and using the Extra Precision (XP) mode, saving 20 maximum number of poses for each compound for the subsequent analysis.

4.2. General synthetic procedures

NMR spectra (^{1}H, ^{13}C) were recorded on a Bruker Avance DRX400, Bruker Avance DRX500, Bruker Avance DRX600 and Varian Inova500 NMR spectrometers at T = 298 K. The compounds were dissolved in 0.5 mL of d-$CHCl_3$ (Aldrich, 99.8+ Atom% D), DMSO-d_6 (Aldrich, 99.8+ Atom% D). Coupling constants (*J*) are reported in Hertz, and chemical shifts (cs) are expressed in parts per million (ppm) on the delta (δ) scale relative to $CHCl_3$ (7.16 ppm for ^{1}H and 77.20 ppm for ^{13}C) or DMSO (2.50 ppm for ^{1}H and 39.52 ppm for ^{13}C) as the internal reference. Multiplicities are reported as follows: s, singlet; d, doublet; t, triplet; m, multiplet; dd, doublet of doublets. ^{13}C DEPTQ experiments (dept polarization transfer with decoupling during acquisition using shaped pulse for 180° pulse on f1 channel) were acquired at 100 MHz or 125 MHz and referenced to the internal solvent signal. High Resolution Mass Spectrometry spectra (HRMS) were performed on a LTQ-Orbitrap XL (Thermo Fisher Scientific, Bremen, Germany) mass spectrometer, with electrospray ionization (ESI). HPLC was performed using a Waters Model 510 pump equipped with Waters Rheodine injector and a differential refractometer, model 401. All the solvents used for the synthesis were HPLC grade; they were purchased from Aldrich and VWR. The reagents for the synthesis were purchased from Sigma Aldrich and Zentek S.r.l. and used as received. Toluene was distilled from calcium hydride immediately prior to use.

Reaction progress was monitored via thin-layer chromatography (TLC) on Alugram® silica gel G/UV254 plates.

4.2.1. Generical procedure a for the synthesis of compounds **1-23**

The synthetic strategy of the targeted molecules involves a one-pot multicomponent reaction as depicted in Scheme 1. 2-amino-1-phenylethanone (1 eq), an excess of 2-mercaptoacetic acid and substituted-benzaldehyde (1 eq) were dissolved in dry toluene (10 mL) and stirred under reflux. The time of reaction and the excess of 2-mercaptoacetic acid used are shown below. After the competition of the reaction, the solvent was evaporated, the mixture was diluted with ethyl acetate and washed with sat. $NaHCO_3$ (10 mL), brine (10 mL) and 0.5 N HCl (10 ml).

The organic lower was dried over anhydrous Na_2SO_4, filter, and concentrated under reduced pressure to afford the crude product. The resulting residue was purified on a silica gel column chromatography in hexane/ethyl acetate and/or with HPLC.

4.2.2. Synthesis of 3-(2-(4-bromophenyl)-2-oxoethyl)-2-(2,6-dichlorophenyl)thiazolidin-4-one (compound **1**)

Compound **1** was obtained following the generical procedure *a* and using 8 equivalents of 2-mercaptoacetic acid (Reaction time: 12 h). Purification by silica gel (95:5 hexane/AcOEt) gave compound **1** (92%) as a white solid. An analytic sample of **1** was obtained through purification with HPLC on a Phenomenex C18 (5 μm; 10 mm i.d. x 250 mm), with MeOH/H_2O (95:5) as eluent (flow rate 3 mL/min) in 25 min (t_R = 5.0 min).

^{1}H NMR (400 MHz, DMSO-d_6, Bruker Avance DRX400) δ 7.91 (d, *J* = 8.5 Hz, 2H), 7.71 (d, *J* = 8.5 Hz, 2H), 7.54 (dd, *J* = 7.8 Hz, 1.3 Hz, 1H), 7.48 (dd, *J* = 8.0 Hz, 1.3 Hz, 1H), 7.42 (t, *J* = 8.0 Hz, 1H), 6.63 (s, 1H), 5.10 (d, *J* = 18.2 Hz, 1H), 4.13 (d, *J* = 18.2 Hz, 1H), 3.91 (s, 2H).

^{13}C NMR (100 MHz, DMSO-d_6, Bruker Avance DRX400) δ 193.3, 171.6, 135.6, 134.8, 133.7, 132.3 (2C), 132.0, 131.7, 131.7, 130.6 (2C), 129.6, 128.7, 58.4, 49.3, 33.7.

HR-MS: *m/z* calcd for $C_{17}H_{12}BrCl_2NO_2S$ $[M+H]^+$445.9129; $[M+Na]^+$467.9006.

m.p. 148–151 °C.

4.2.3. Synthesis of 2-(2,4-dichlorophenyl)-3-(2-(4-methoxyphenyl)-2-oxoethyl)thiazolidin-4-one (compound **2**)

Compound **2** was obtained following the generical procedure *a* and using 34 equivalents of 2-mercaptoacetic acid (Reaction time: 72 h). Purification by silica gel (8:2 hexane/AcOEt) gave compound **2** (95%) as a colorless oil. An analytic sample of **2** was obtained through purification with HPLC with hexane/acetate (40:60) as eluent (flow rate 3 mL/min) in 25 min (t_R = 5.5 min).

^{1}H NMR (400 MHz, DMSO-d_6, Bruker Avance DRX400) δ 7.98 (d, *J* = 6.7 Hz, 2H), 7.58 (d, *J* = 6.2 Hz, 2H), 7.56–7.41 (m, 3H), 6.62 (s, 1H), 5.10 (d, *J* = 18.2 Hz, 1H), 4.14 (d, *J* = 18.2 Hz, 1H), 3.91 (s, 2H).

^{13}C NMR (100 MHz, DMSO-d_6, Bruker Avance DRX400) δ 192.8, 171.1, 139.0, 135.1, 134.3, 132.9, 131.5, 131.3, 131.2, 130.0 (2C), 129.1, 128.9 (2C), 57.9, 48.8, 32.7.

HR-MS: *m/z* calcd for $C_{17}H_{12}Cl_3NO_2S$ $[M+H]^+$401.9654; found $[M+Na]^+$423.9598.

4.2.4. Synthesis of 3-(2-(4-bromophenyl)-2-oxoethyl)-2-(3,5-dibromo-4-hydroxyphenyl)thiazolidin-4-one (compound **3**)

Compound **3** was obtained following the generical procedure *a* and using 8 equivalents of 2-mercaptoacetic acid (Reaction time: 24 h). Purification by silica gel (9:1 hexane/AcOEt) gave compound **3** (89%) as a white powder. An analytic sample of **3** was obtained through purification with HPLC on a Nucleodur 100–5 (5 μm; 10 mm i.d. x 250 mm), with hexane/AcOEt (40:60) as eluent (flow rate 3 mL/min) in 25 min (t_R = 6.0 min).

^{1}H NMR (400 MHz, DMSO-d_6, Bruker Avance DRX400) δ 7.88 (d, *J* = 8.4 Hz, 2H), 7.73 (d, *J* = 8.3 Hz, 2H), 7.59 (s, 2H), 5.69 (s, 1H), 4.94 (d, *J* = 15.4 Hz, 1H), 4.25 (d, *J* = 14.3 Hz, 1H), 4.02 (d, *J* = 15.6 Hz, 1H) 3.74 (d, *J* = 15.6 Hz, 1H).

^{13}C NMR (100 MHz, DMSO-d_6, Bruker Avance DRX400) δ 192.7, 171.6, 151.4, 134.2, 133.7, 132.0 (2C), 131.5 (2C), 130.2 (2C), 128.2, 112.1 (2C), 61.1, 49.5, 32.3.

HR-MS: *m/z* calcd for $C_{17}H_{12}Br_3NO_3S$ $[M+H]^+$ 551.8047; found $[M+Na]^+$ 573.7986.

m.p. 139–142 °C.

4.2.5. Synthesis of 2-(3,5-dibromo-4-hydroxyphenyl)-3-(2-(4-methoxyphenyl)-2-oxoethyl)thiazolidin-4-one (compound **4**)

Compound **4** was obtained following the generical procedure *a* and using 8 equivalents of 2-mercaptoacetic acid (Reaction time: 12 h). Purification by silica gel (8:2 hexane/AcOEt) gave compound **4** (86%) as a white solid.

^{1}H NMR (400 MHz, DMSO-d_6, Bruker Avance DRX400) δ 7.92 (d, *J* = 8.7 Hz, 2H), 7.58 (s, 2H), 7.02 (d, *J* = 8.7 Hz, 2H), 5.70 (s, 1H), 4.93 (d, *J* = 18.0 Hz, 1H), 4.16 (d, *J* = 18.0 Hz, 1H), 4.00 (d, *J* = 15.6 Hz, 1H), 3.83 (s, 3H), 3.71 (d, *J* = 15.6 Hz, 1H).

^{13}C NMR (100 MHz, DMSO-d_6, Bruker Avance DRX400) δ 191.2, 171.4, 163.7, 151.3, 133.9, 131.6 (2C), 130.5 (2C), 127.5, 114.1 (2C), 112.1 (2C), 61.6, 55.5, 48.9, 31.8.

HR-MS: *m/z* calcd for $C_{18}H_{15}Br_2NO_4S$ $[M+H]^+$501.9068; found $[M+Na]^+$523.8943.

m.p. 127–131 °C.

4.2.6. Synthesis of 3-(2-(4-bromophenyl)-2-oxoethyl)-2-(3-chloro-5-fluoro-4-hydroxyphenyl)thiazolidin-4-one (compound 5)

Compound **5** was obtained following the generical procedure *a* and using 16 equivalents of 2-mercaptoacetic acid (Reaction time: 24 h). Purification by silica gel (85:15 hexane/AcOEt) gave compound **5** (77%) as a white oil. An analytic sample of **5** was obtained through purification with HPLC on a Nucleodur 100–5 (5 μm; 10 mm i.d. x 250 mm), with hexane/AcOEt (40:60) as eluent (flow rate 3 mL/min) in 25 min (t_R = 6.0 min).

^{1}H NMR (400 MHz, DMSO-d_6, Bruker Avance DRX400) δ 7.88 (d, J = 8.5 Hz, 2H), 7.73 (d, J = 8.5 Hz, 2H), 7.28 (s, 2H), 5.71 (s, 1H), 4.95 (d, J = 18.2 Hz, 1H), 4.25 (d, J = 18.2 Hz, 1H), 4.06 (d, J = 15.6 Hz, 1H), 3.74 (d, J = 15.6 Hz, 1H).

^{13}C NMR (100 MHz, DMSO-d_6, Bruker Avance DRX400) δ 192.1, 171.1, 152.2 (d, J = 242.6 Hz), 141.9 (d, J = 16.5 Hz), 133.5, 131.9 (2C), 131.4 (d, J = 6.4 Hz), 130.1 (2C), 128.0, 124.4, 121.9 (d, J = 4.5 Hz), 114.8 (d, J = 20.0 Hz), 61.8, 49.11, 31.08.

HR-MS: *m/z* calcd for $C_{17}H_{12}BrClFNO_3S$ $[M+H]^+$445.9394; found $[M+Na]^+$467.9250.

4.2.7. Synthesis of 2-(3-chloro-5-fluoro-4-hydroxyphenyl)-3-(2-(4-methoxyphenyl)-2-oxoethyl)thiazolidin-4-one (compound 6)

Compound **6** was obtained following the generical procedure *a* and using 8 equivalents of 2-mercaptoacetic acid (Reaction time: 24 h). Purification by silica gel (8:2 hexane/AcOEt) gave compound **6** (90%) as a white solid.

^{1}H NMR (400 MHz, DMSO-d_6, Bruker Avance DRX400) δ 7.97 (d, J = 6.8 Hz, 2H), 7.32 (s, 2H), 7.06 (d, J = 8.9 Hz, 1H), 5.75 (s, 1H), 4.98 (d, J = 18.0 Hz, 1H), 4.18 (d, J = 6.5 Hz, 1H), 4.04 (dd, J = 15.6 Hz, 18 Hz, 1H), 3.87 (s, 3H), 3.80 (d, J = 6.8 Hz, 1H).

^{13}C NMR (100 MHz, DMSO-d_6, Bruker Avance DRX400) δ 191.2, 171.1, 163.6, 151.9 (d, J = 242.7 Hz), 141.9 (d, J = 16.5 Hz), 131.5 (d, J = 6.4 Hz), 130.5 (2C), 127.4, 124.4 (d, J = 2.0 Hz), 121.9 (d, J = 4.4 Hz). 114.0 (2C), 114.0 (d, J = 7.3 Hz), 66.6, 60.5, 53.8, 36.4.

HR-MS: *m/z* calcd for $C_{18}H_{15}ClFNO_4S$ $[M+H]^+$ 396.0394; found $[M+H]^+$ 396.0378.

m.p. 128–131 °C.

4.2.8. Synthesis of 2-(3-bromo-5-fluoro-4-hydroxyphenyl)-3-(2-(4-methoxyphenyl)-2-oxoethyl)thiazolidin-4-one (compound 7)

Compound **7** was obtained following the generical procedure *a* and using 8 equivalents of 2-mercaptoacetic acid (Reaction time: 24 h). Purification by silica gel (8:2 hexane/AcOEt) gave compound **7** (89%) a white solid. An analytic sample of **7** was obtained through purification with HPLC on a Nucleodur 100–5 (5 μm; 10 mm i.d. x 250 mm), with hexane/AcOEt (40:60) as eluent (flow rate 3 mL/min) in 25 min (t_R = 8.5 min).

^{1}H NMR (500 MHz, $CDCl_3$, Varian Inova 500) δ 7.85 (d, J = 8.8 Hz, 2H), 7.25 (s, 1H), 7.10 (d, J = 10.3 Hz, 2H), 6.92 (d, J = 8.7 Hz, 1H), 5.82 (s, 1H), 5.19 (d, J = 17.6 Hz, 1H), 3.92–3.80 (m, 3H).3.82 (s, 3H).

^{13}C NMR (100 MHz, DMSO-d_6, Bruker Avance DRX400) δ 191.1, 171.0, 163.6, 151.6 (d, J = 243.2 Hz), 144.4, 131.6, 130.3 (2C), 127.3, 127.1, 114.4, (d, J = 20.3 Hz), 113.8 (2C), 111.7 (d, J = 14.0 Hz), 61.8, 55.5, 48.7, 31.7.

m.p. 138–144 °C.

HR-MS: *m/z* calcd for $C_{18}H_{15}BrFNO_4S$ $[M+H]^+$439.9889; found $[M+H]^+$ 439.9982.

4.2.9. Synthesis of 3-(2-(4-chlorophenyl)-2-oxoethyl)-2-(3-fluoro-4-hydroxy-5-methoxyphenyl)thiazolidin-4-one (compound 8)

Compound **8** was obtained following the generical procedure *a* and using 24 equivalents of 2-mercaptoacetic acid (Reaction time: 72 h). Purification by silica gel (85:15 hexane/AcOEt) gave compound **8** (74%) as an orange solid.

^{1}H NMR (400 MHz, DMSO-d_6, Bruker Avance DRX400) δ 7.97 (d, J = 10.0 Hz, 2H), 7.59 (d, J = 9.8 Hz, 2H), 6.87 (d, J = 1.9 Hz, 1H), 6.84 (s, 1H), 5.73 (s, 1H), 5.00 (d, J = 18.7 Hz, 1H), 4.19 (d, J = 18.7 Hz, 1H), 3.99 (d, J = 9.7 Hz, 1H), 3.93 (d, J = 9.7 Hz, 1H), 3.77 (s, 3H).

^{13}C NMR (100 MHz, DMSO-d_6, Bruker Avance DRX400) δ 192.3, 171.4, 170.6, 151.2 (d, J = 238.7 Hz), 149.5 (d, J = 6.4 Hz), 138.8, 134.8 (d, J = 14.2 Hz), 133.2, 130.3 (2C), 129.9 (2C), 129.5 (d, J = 7.7 Hz), 128.9 (2C), 107.7 (d, J = 20.3 Hz), 107.1, 62.6, 56.1, 49.2, 31.7.

HR-MS: *m/z* calcd for $C_{18}H_{15}ClFNO_4S$ $[M+H]^+$396.0394; found $[M+Na]^+$ 418.1628.

m.p. 133–137 °C.

4.2.10. Synthesis of 3-(2-(4-bromophenyl)-2-oxoethyl)-2-(4-hydroxy-3-(trifluoromethyl)phenyl)thiazolidin-4-one (compound 9)

Compound **9** was obtained following the generical procedure *a* and using 16 equivalents of 2-mercaptoacetic acid (Reaction time: 24 h). Purification by silica gel (85:15 hexane/AcOEt) gave compound **9** (71%) as a yellow oil. An analytic sample of **9** was obtained through purification with HPLC on a Nucleodur 100–5 (5 μm; 10 mm i.d. x 250 mm), with hexane/AcOEt (40:60) as eluent (flow rate 3 mL/min) in 25 min (t_R = 9.0 min).

^{1}H NMR (500 MHz, $CDCl_3$, Varian Inova 500) δ 7.64 (d, J = 8.5 Hz, 2H), 7.53 (d, J = 8.5 Hz, 2H), 7.42 (s, 1H), 7.34 (m, 1H), 6.90 (d, J = 8.4 Hz, 1H), 5.81 (s, 1H), 5.05 (d, J = 17.8 Hz, 1H), 3.85 (d, J = 15.8 Hz, 1H), 3.78 (m, 2H).

^{13}C NMR (125 MHz, $CDCl_3$, Varian Inova 500) δ 193.9, 172.3, 155.4, 133.3, 133.1, 132.4 (2C), 132.3, 129.6 (2C), 126.7, 126.6 (q, J = 103.6 Hz), 119.09, 118.0 (q, J = 52.2 Hz), 118.4, 63.5, 52.8, 33.5.

HR-MS: *m/z* calcd for $C_{18}H_{13}BrF_3NO_3S$ $[M+ H]^+$ 461.9752; found $[M+Na]^+$ 483.9687.

4.2.11. Synthesis of 2-(4-hydroxy-3-(trifluoromethyl)phenyl)-3-(2-(4-methoxyphenyl)-2-oxoethyl)thiazolidin-4-one (compound 10)

Compound **10** was obtained following the generical procedure *a* and using 16 equivalents of 2-mercaptoacetic acid (Reaction time: 24 h). Purification by silica gel (8:2 hexane/AcOEt) gave compound **10** (88%) as a yellow oil. An analytic sample of **10** was obtained through purification with HPLC on a Nucleodur 100–5 (5 μm; 10 mm i.d. x 250 mm), with hexane/AcOEt (40:60) as eluent (flow rate 3 mL/min) in 25 min (t_R = 13.0 min).

^{1}H NMR (500 MHz, $CDCl_3$, Varian Inova 500) δ 7.84 (d, J = 8.9 Hz, 2H), 7.49 (s, 1H), 7.42 (d, J = 8.3 Hz, 1H), 6.97 (d, J = 8.3 Hz, 1H), 6.91 (d, J = 8.9 Hz, 2H), 5.90 (s, 1H), 5.15 (d, J = 17.5 Hz, 1H), 3.91 (d, J = 17.0 Hz, 1H), 3.86 (s, 3H), 3.83 (d, J = 8.2 Hz, 2H).

^{13}C NMR (100 MHz, DMSO-d_6, Bruker Avance DRX400) δ 191.4, 171.4, 169.3, 164.0, 156.3, 133.5, 130.2 (2C), 128.5 (q, J = 129.7 Hz), 126.5, 121.8 (q, J = 96.5 Hz), 117.4, 114.1 (2C), 62.2, 55.5, 48.8, 31.8.

HR-MS: *m/z* calcd for $C_{19}H_{16}F_3NO_4S$ $[M+H]^+$ 412.0752; found $[M+H]^+$ 412.0635.

4.2.12. Synthesis of 3-(2-(4-fluorophenyl)-2-oxoethyl)-2-(4-hydroxy-3-(trifluoromethyl)phenyl)thiazolidin-4-one (compound 11)

Compound **11** was obtained following the generical procedure *a* and using 16 equivalents of 2-mercaptoacetic acid (Reaction time: 12 h). Purification by silica gel (8:2 hexane/AcOEt) gave compound **11** (62%) as a colorless oil. An analytic sample of **11** was obtained through purification with HPLC on a Nucleodur 100–5 (5 μm; 10 mm i.d. x 250 mm), with hexane/AcOEt (40:60) as eluent (flow rate 3 mL/min) in 25 min (t_R = 10.0 min).

^{1}H NMR (500 MHz, $CDCl_3$, Varian Inova 500) δ 8.06–7.99 (m, 2H), 7.54 (s, 1H), 7.52 (d, J = 8.5 Hz, 1H), 7.33 (t, J = 8.8 Hz, 1H), 7.01 (d, J = 8.3 Hz, 2H), 5.79 (s, 1H), 4.95 (d, J = 18.1 Hz, 1H), 3.90–3.35 (m, 3H).

^{13}C NMR (100 MHz, DMSO-d_6, Bruker Avance DRX400) δ 191.4, 171.0, 160.1 (d, J = 250.8 Hz), 144.2, 132.8, 130.7 (d, J = 5.2 Hz, 2C),

128.5, 126.2, 123.7, 117.3, 115.8 (d, $J = 8.9$ Hz, 2C), 110.7 (q, $J = 129.0$ Hz), 73.7 (q, $J = 55.6$ Hz), 61.9, 48.9, 31.9.

HR-MS: *m/z* calcd for $C_{18}H_{13}F_4NO_3S$ $[M+H]^+$400.0552, found $[M+H]^+$ 400.0536.

4.2.13. Synthesis of 3-(2-(4-bromophenyl)-2-oxoethyl)-2-(4-chlorophenyl) thiazolidin-4-one (compound **12**)

Compound **12** was obtained following the generical procedure *a* and using 16 equivalents of 2-mercaptoacetic acid (Reaction time: 24 h). Purification by silica gel (9:1 hexane/AcOEt) gave compound **12** (87%) as a white oil. An analytic sample of **12** was obtained through purification with HPLC on a Nucleodur 100–5 (5 μm; 10 mm i.d. x 250 mm), with hexane/AcOEt (40:60) as eluent (flow rate 3 mL/min) in 25 min (t_R = 12.0 min).

^{1}H NMR (400 MHz, $CDCl_3$, Bruker Avance DRX400) δ 7.63 (d, $J = 8.6$ Hz, 2H), 7.52 (d, $J = 8.6$ Hz, 2H), 7.28 (d, $J = 7.9$ Hz, 2H), 7.21 (d, $J = 7.9$ Hz, 2H), 5.80 (s, 1H), 5.07 (d, $J = 17.8$ Hz, 1H), 3.81–3.79 (m, 1H), 3.75 (d, $J = 7.0$ Hz, 1H).

^{13}C NMR (100 MHz, $CDCl_3$, Bruker Avance DRX400) δ 191.9, 172.5, 136.5, 135.5, 133.2, 133.2, 132.2 (2C), 129.5 (2C), 129.4 (2C), 129.2 (2C), 63.3, 48.6, 29.8.

HR-MS: *m/z* calcd for $C_{17}H_{13}BrClNO_2S$ $[M+H]^+$ 411.9539; found $[M+K]^+$ 450.9351.

4.2.14. Synthesis of 2-(4-chlorophenyl)-3-(2-(4-methoxyphenyl)-2-oxoethyl)thiazolidin-4-one (compound **13**)

Compound **13** was obtained following the generical procedure *a* and using 24 equivalents of 2-mercaptoacetic acid (Reaction time: 48 h). Purification by silica gel (9:1 hexane/AcOEt) gave compound **13** (73%) as a white oil. An analytic sample of **13** was obtained through purification with HPLC on a Nucleodur 100–5 (5 μm; 10 mm i.d. x 250 mm), with hexane/AcOEt (40:60) as eluent (flow rate 3 mL/min) in 25 min (t_R = 8.5 min).

^{1}H NMR (400 MHz, $CDCl_3$, Bruker Avance DRX400) δ 7.76 (d, $J = 8.9$ Hz, 2H), 7.28 (d, $J = 8.2$ Hz, 2H), 7.23 (d, $J = 8.1$ Hz, 2H), 6.84 (d, $J = 8.8$ Hz, 2H), 5.85 (s, 1H), 5.11 (d, $J = 17.4$ Hz, 1H), 3.86–3.71 (m, 6H).

^{13}C NMR (100 MHz, $CDCl_3$, Bruker Avance DRX400) δ 191.1, 172.3, 164.3, 136.9, 135.8, 130.5 (2C), 129.6 (2C), 129.4 (2C), 127.8, 114.2 (2C), 63.9, 56.2, 48.8, 33.0.

HR-MS: *m/z* calcd for $C_{18}H_{16}ClNO_3S$ $[M+H]^+$362.0539; found $[M+H]^+$ 362.0484.

4.2.15. Synthesis of 3-(2-(4-methoxyphenyl)-2-oxoethyl)-2-(p-tolyl) thiazolidin-4-one (compound **14**)

Compound **14** was obtained following the generical procedure *a* and using 48 equivalents of 2-mercaptoacetic acid (Reaction time: 120 h). Purification by silica gel (9:1 hexane/AcOEt) gave compound **14** (78%) as a yellow oil. An analytic sample of **14** was obtained through purification with HPLC on a Nucleodur 100–5 (5 μm; 10 mm i.d. x 250 mm), with hexane/AcOEt (40:60) as eluent (flow rate 3 mL/min) in 25 min (t_R = 8.0 min).

^{1}H NMR (400 MHz, $CDCl_3$, Bruker Avance DRX400) δ 7.84 (d, $J = 8.7$ Hz, 2H), 7.25 (d, $J = 7.6$ Hz, 2H), 7.19 (d, $J = 7.7$ Hz, 2H), 6.91 (d, $J = 8.8$ Hz, 2H), 5.91 (s, 1H), 5.18 (d, $J = 17.6$ Hz, 1H), 3.87 (s, 3H), 3.91–3.82 (m, 3H), 2.37 (s, 3H).

^{13}C NMR (100 MHz, $CDCl_3$, Bruker Avance DRX400) δ 191.2, 172.2, 164.1, 139.5 (2C), 135.1, 130.7 (2C), 129.8 (2C), 127.9 (2C), 113.9 (2C), 63.9, 55.5, 47.8, 32.9, 21.4.

HR-MS: *m/z* calcd for $C_{19}H_{19}NO_3S$ $[M+H]^+$ 341.1086; found $[M+Na]^+$ 364.0979.

4.2.16. Synthesis of 3-(2-(4-bromophenyl)-2-oxoethyl)-2-(2-chloro-4-methylphenyl)thiazolidin-4-one (compound **15**)

Compound **15** was obtained following the generical procedure *a* and using 48 equivalents of 2-mercaptoacetic acid (Reaction time: 120 h). Purification by silica gel (9:1 hexane/AcOEt) gave compound **15** (91%) as a yellow oil. An analytic sample of **15** was obtained through purification with HPLC on a Nucleodur 100–5 (5 μm; 10 mm i.d. x 250 mm), with hexane/AcOEt (40:60) as eluent (flow rate 3 mL/min) in 25 min (t_R = 6.5 min).

^{1}H NMR (400 MHz, $CDCl_3$, Bruker Avance DRX400) δ 7.76 (d, $J = 8.6$ Hz, 2H), 7.61 (d, $J = 8.5$ Hz, 2H), 7.29 (m, 2H), 7.15 (d, $J = 7.8$ Hz, 1H), 6.29 (s, 1H), 5.11 (d, $J = 17.7$ Hz, 1H), 3.94 (d, $J = 17.7$ Hz, 1H), 3.86 (m, 2H), 2.26 (s, 3H).

^{13}C NMR (100 MHz, $CDCl_3$, Bruker Avance DRX400) δ 192.1, 172.7, 140.9, 133.5, 133.4, 132.8, 132.4 (2C), 131.0, 129.7 (2C), 129.4, 128.8, 128.5, 60.5, 49.2, 32.0, 20.6.

HR-MS: *m/z* calcd for $C_{18}H_{15}BrClNO_2S$ $[M+H]^+$425.9695; found $[M+H]^+$426.0074.

4.2.17. Synthesis of 2-(2-chloro-4-methylphenyl)-3-(2-(4-methoxyphenyl)-2-oxoethyl)thiazolidin-4-one (compound **16**)

Compound **16** was obtained following the generical procedure *a* and using 32 equivalents of 2-mercaptoacetic acid (Reaction time: 48 h). Purification by silica gel (85:15 hexane/AcOEt) gave compound **16** (90%) as a white oil. An analytic sample of **16** was obtained through purification with HPLC on a Nucleodur 100–5 (5 μm; 10 mm i.d. x 250 mm), with hexane/AcOEt (40:60) as eluent (flow rate 3 mL/min)) in 25 min (t_R = 8.5 min).

^{1}H NMR (400 MHz, $CDCl_3$, Bruker Avance DRX400) δ 7.80 (d, $J = 8.3$ Hz, 2H), 7.21 (d, $J = 7.8$ Hz, 1H), 7.12 (s, 1H), 7.06 (d, $J = 7.7$ Hz, 1H), 6.84 (d, $J = 8.2$ Hz, 2H), 6.23 (s, 1H), 5.15 (d, $J = 17.5$ Hz, 1H), 3.86 (d, $J = 17.5$ Hz, 1H), 3.79 (s, 3H), 3.77 (d, $J = 6.0$ Hz, 2H), 2.27 (s, 3H).

^{13}C NMR (100 MHz, $CDCl_3$, Bruker Avance DRX400) δ 191.0, 172.8, 164.6, 141.0, 140.7, 133.2, 130.9, 130.6, 130.5 (2C), 128.7, 127.9, 114.4 (2C), 60.5, 55.5, 48.8, 32.7, 21.6.

HR-MS: *m/z* calcd for $C_{19}H_{18}ClNO_3S$ $[M+H]^+$ 376.0696; found $[M+H]^+$ 376.0687.

4.2.18. Synthesis of 2-(2-chloro-4-hydroxyphenyl)-3-(2-(4-methoxyphenyl)-2-oxoethyl)thiazolidin-4-one (compound **17**)

Compound **17** was obtained following the generical procedure *a* and using 24 equivalents of 2-mercaptoacetic acid (Reaction time: 12 h). Purification by silica gel (9:1 hexane/AcOEt) gave compound **17** (58%) as a yellow solid. An analytic sample of **17** was obtained through purification with HPLC on a Nucleodur 100–5 (5 μm; 10 mm i.d. x 250 mm), with hexane/AcOEt (40:60) as eluent (flow rate 3 mL/min) in 25 min (t_R = 9.0 min).

^{1}H NMR (600 MHz, $CDCl_3$, Bruker Avance DRX600) δ 7.80 (d, $J = 8.0$ Hz, 2H), 7.23 (d, $J = 7.7$ Hz, 1H), 7.09 (d, $J = 7.7$ Hz, 1H), 6.84 (d, $J = 8.0$ Hz, 2H), 6.31 (s, 1H), 5.25 (d, $J = 17.5$ Hz, 1H), 3.87 (d, $J = 17.5$ Hz, 1H), 3.76 (m, 5H).

^{13}C NMR (150 MHz, $CDCl_3$, Bruker Avance DRX600) δ 191.0, 172.6, 164.2, 149.9, 130.5 (2C), 129.8, 127.8, 127.0, 126.3, 121.4, 121.2, 114.1 (2C), 59.0, 55.3, 48.7, 32.5.

HR-MS: *m/z* calcd for $C_{18}H_{16}ClNO_4S$ $[M+H]^+$378.0532; found $[M+Na]^+$400.0381.

m.p. 150–153 °C.

4.2.19. Synthesis of 2-(2,4-dichlorophenyl)-3-(2-(4-methoxyphenyl)-2-oxoethyl)thiazolidin-4-one (compound **18**)

Compound **18** was obtained following the generical procedure *a* and using 32 equivalents of 2-mercaptoacetic acid (Reaction time: 72 h). Purification by silica gel (85:15 hexane/AcOEt) gave compound **18** (91%) as a yellow oil.

^{1}H NMR (400 MHz, DMSO-d_6, Bruker Avance DRX400) δ 7.94 (d, $J = 8.9$ Hz, 2H), 7.66 (d, $J = 2.0$ Hz, 1H), 7.51–7.44 (m, 2H), 7.03 (d, $J = 8.9$ Hz, 2H), 6.04 (s, 1H), 5.11 (d, $J = 18.0$ Hz, 1H), 4.26 (d, $J = 18.0$ Hz, 1H), 3.88 (d, $J = 15.8$ Hz, 1H), 3.84 (s, 3H), 3.77 (d, $J = 15.8$ Hz, 1H).

^{13}C NMR (100 MHz, DMSO-d_6, Bruker Avance DRX400) δ 191.2, 171.8, 163.7, 136.4, 133.7, 133.0, 130.4 (2C), 129.4, 128.1 (2C), 127.4, 114.1 (2C), 59.2, 55.8, 49.5, 31.4.

HR-MS: *m/z* calcd for $C_{18}H_{15}Cl_2NO_3S$ $[M+H]^+$ 396.0150; found $[M+Na]^+$418.0041.

4.2.20. Synthesis of 3-(2-(4-bromophenyl)-2-oxoethyl)-2-(4-(dimethylamino)phenyl)thiazolidin-4-one (compound **19**)

Compound **19** was obtained following the generical procedure *a* and using 32 equivalents of 2-mercaptoacetic acid (Reaction time: 72 h). Pure compound **19** (brown oil) was obtained through purification with HPLC on a Nucleodur 100–5 (5 μm; 10 mm i.d. x 250 mm), with hexane/AcOEt (40:60) as eluent (flow rate 3 mL/min) in 25 min (t_R = 7.0 min) (Yied = 45%).

^{1}H NMR (400 MHz, $CDCl_3$, Bruker Avance DRX400) δ 7.63 (d, J = 8.4 Hz, 2H), 7.51 (d, J = 8.3 Hz, 2H), 7.12 (d, J = 8.5 Hz, 2H), 6.59 (d, J = 8.5 Hz, 2H), 5.78 (s, 1H), 5.02 (d, J = 17.7 Hz, 1H), 3.84–3.81 (m, 2H), 3.73 (d, J = 17.5 Hz, 1H), 2.90 (s, 6H).

^{13}C NMR (100 MHz, $CDCl_3$, Bruker Avance DRX400) δ 190.7, 172.4, 147.2, 132.7 (2C), 129.7 (2C), 124.8 (2C), 117.7 (2C), 114.3 (2C), 63.8, 51.4, 43.8 (2C), 32.7.

HR-MS: *m/z* calcd for $C_{19}H_{19}BrN_2O_2S$ $[M+H]^+$ 419.0351; found $[M+Na]^+$442.0286.

4.2.21. Synthesis of 2-(4-(dimethylamino)phenyl)-3-(2-(4-methoxyphenyl)-2-oxoethyl)thiazolidin-4-one (compound **20**)

Compound **20** was obtained following the generical procedure *a* and using 24 equivalents of 2-mercaptoacetic acid (Reaction time: 72 h). Pure compound **20** (orange oil) was obtained through purification with HPLC on a Nucleodur 100–5 (5 μm; 10 mm i.d. x 250 mm), with hexane/AcOEt (40:60) as eluent (flow rate 3 mL/min) in 25 min (t_R = 9.0 min) (Yied = 49%).

^{1}H NMR (400 MHz, $CDCl_3$, Bruker Avance DRX400) δ 7.75 (d, J = 8.7 Hz, 2H), 7.32 (d, J = 8.7 Hz, 2H), 7.16 (d, J = 8.3 Hz, 2H), 6.83 (d, J = 8.3 Hz, 2H), 5.85 (s, *1*H), 5.09 (d, J = 17.6 Hz, 1H), 3.80 (m, 3H), 3.78 (s, 3H), 3.03 (s, 6H).

^{13}C NMR (100 MHz, $CDCl_3$, Bruker Avance DRX400) δ 190.7, 172.4, 164.0, 147.4, 133.8, 130.5 (2C), 129.6 (2C), 117.7 (2C), 114.3 (2C), 63.9, 55.6, 51.3, 43.8 (2C), 32.7.

HR-MS: *m/z* calcd for $C_{20}H_{22}N_2O_3S$ $[M+H]^+$ 370.1371; found $[M+Na]^+$393.1236.

m.p. 153–154 °C.

4.2.22. Synthesis of 3-(2-(4-bromophenyl)-2-oxoethyl)-2-(3-((2-chlorobenzyl)oxy)-4-methoxyphenyl)thiazolidin-4-one (compound **21**)

Compound **21** was obtained following the generical procedure *a* and using 8 equivalents of 2-mercaptoacetic acid (Reaction time: 12 h). Purification by silica gel (85:15 hexane/AcOEt) gave compound **21** (68%) as a white solid. An analytic sample of **21** was obtained through purification with HPLC on a Phenomenex C18 (5 μm; 10 mm i.d. x 250 mm), with MeOH/H_2O (95:5) as eluent (flow rate 3 mL/min) in 25 min (t_R = 5.0 min).

^{1}H NMR (500 MHz, $CDCl_3$, Varian Inova500) δ 7.59 (d, J = 8.4 Hz, 2H), 7.51 (d, J = 8.6 Hz, 2H), 7.32 (d, J = 2.3 Hz, 1H), 7.20 (dd, J = 7.6 Hz, 2.3 Hz, 1H), 7.17–6.81 (m, 5H), 5.74 (s, 1H), 5.23 (d, J = 5.1 Hz, 2H), 4.99 (d, J = 17.7 Hz, 1H), 3.89 (s, 3H), 3.87 (d, J = 17.6 Hz, 2H), 3.76 (t, J = 17.1 Hz, 2H).

^{13}C NMR (125 MHz, $CDCl_3$, Varian Inova500) δ 193.7, 172.1, 149.2, 147.7, 135.3, 134.1, 133.2, 132.2 (2C), 131.5 (2C), 129.8, 129.5, 129.3, 126.8, 121.3, 113.7, 112.9, 70.2, 62.1, 55.9, 51.7, 33.3.

HR-MS: *m/z* calcd for $C_{25}H_{21}BrClNO_4S$ $[M+H]^+$ 548.0063; found $[M+K]^+$570.0099.

m.p. 153–154 °C.

4.2.23. Synthesis of 2-(3-((2-chloro-6-fluorobenzyl)oxy)-4-methoxyphenyl)-3-(2-(4-chlorophenyl)-2-oxoethyl)thiazolidin-4-one (compound **22**)

Compound **22** was obtained following the generical procedure *a* and using 16 equivalents of 2-mercaptoacetic acid (Reaction time: 72 h). Purification by silica gel (9:1 hexane/AcOEt) gave compound **22** (89%) as a white solid.

^{1}H NMR (400 MHz, $CDCl_3$, Bruker Avance DRX400) δ 7.61 (d, J = 8.3 Hz, 2H), 7.45 (d, J = 8.2 Hz, 2H), 7.31–7.23 (m, *2*H), 7.15–7.08 (m, 2H), 6.87 (s, 1H), 6.84 (t, J = 8.6 Hz, 1H), 6.73 (d, J = 8.1 Hz, 1H), 5.67 (s, 1H), 5.25 (s, 2H), 5.10 (d, J = 17.8 Hz, 1H), 3.73 (dd, J = 15.3 Hz, 6.3 Hz, 2H), 3.69–3.61 (m, 4H).

^{13}C NMR (100 MHz, $CDCl_3$, Bruker Avance DRX400) δ 191.9, 172.2, 164.2, 161.0, 150.0 (d, J = 280.3 Hz), 140.8, 136.5 (d, J = 5.1 Hz), 130.7 (d, J = 9.9 Hz), 129.4 (2C), 129.2 (2C) 125.6 (d, J = 3.6 Hz), 122.3 (d, J = 5.8 Hz), 122.1, 114.4, 114.3, 111.8, 64.2, 62.9, 55.9, 48.8, 32.9.

HR-MS: *m/z* calcd for $C_{25}H_{20}Cl_2FNO_4S$ $[M+H]^+$ 520.0474; found $[M+H]^+$520.0500.

m.p. 149–152 °C.

4.2.24. Synthesis of 2-(3-((2-chloro-6-fluorobenzyl)oxy)-4-methoxyphenyl)-3-(2-(4-fluorophenyl)-2-oxoethyl)thiazolidin-4-one (compound **23**)

Compound **23** was obtained following the generical procedure *a* and using 16 equivalents of 2-mercaptoacetic acid (Reaction time: 72 h). Purification by silica gel (85:15 hexane/AcOEt) gave compound **23** (84%) as an orange solid.

^{1}H NMR (400 MHz, $CDCl_3$, Bruker Avance DRX400) δ 7.86 (dd, J = 8.6 Hz, 5.4 Hz, 2H), 7.28–7.23 (m, 1H), 7.20 (d, J = 8.0 Hz, 1H), 7.10 (t, J = 8.5 Hz, 2H), 7.04 (d, J = 1.6 Hz, 1H), 6.99 (t, J = 8.6 Hz, 1H), 6.89 (d, J = 8.3 Hz, 1H), 6.79 (d, J = 8.2 Hz, 1H), 5.84 (s, 1H), 5.21 (s, 2H), 5.07 (d, J = 17.7 Hz, 1H), 3.89 (d, J = 14.1 Hz, 1H), 3.85–3.77 (m, 5H).

^{13}C NMR (100 MHz, DMSO-d_6, Bruker Avance DRX400) δ 191.6, 171.2, 165.4 (d, J = 252.8 Hz), 161.5 (d, J = 250.1 Hz), 149.9, 147.6, 135.5 (d, J = 5.1 Hz), 131.8 (d, J = 9.8 Hz), 131.2 (d, J = 2.5 Hz), 131.1, 131.0 (d, J = 9.4 Hz) (2C), 125.7 (d, J = 2.8 Hz), 121.9 (d, J = 10.2 Hz), 121.2, 115.9 (d, J = 22.0 Hz) (2C), 114.7 (d, J = 22.4 Hz), 113.0, 112.0, 62.8, 61.5, 55.5, 49.1, 31.7.

HR-MS: *m/z* calcd for $C_{25}H_{20}ClF_2NO_4S$ $[M+H]^+$ 504,070; found $[M+Na]^+$526.0657.

m.p. 129–134 °C.

4.3. Biological assays

4.3.1. Cell-free mPGES-1 activity assay

mPGES-1 in microsomes of A549 cells was used as enzyme source, as described elsewhere [39]. In brief, A549 cells were stimulated with IL-1β (2 ng/mL) for 48 h, harvested and then sonicated. The lysate was first centrifugated at 10,000×*g* for 10 min, and then at 174,000×*g* for 1 h at 4°C. The pellet (microsomal fraction) was resuspended in 1 ml homogenization buffer (0.1 M potassium phosphate buffer, pH 7.4, 1 mM phenylmethanesulfonyl fluoride, 60 μg/mL soybean trypsin inhibitor, 1 μg/mL leupeptin, 2.5 mM GSH, and 250 mM sucrose), the total protein concentration was determined, and microsomes were diluted in potassium phosphate buffer (0.1 M, pH 7.4) containing GSH (2.5 mM) and seeded in a 96-well plate. Compounds **1–23** or MK-886 (as reference compound) or DMSO (1%) were preincubated with the enzyme for 15 min on ice, and the reactions were triggered by adding 20 μM of PGH_2. After 1 min, the addition of 100 μl of a stop solution (40 mM $FeCl_3$, 80 mM citric acid, and 10 μM 11β-PGE_2) blocked the reaction. PGE_2 and 11β-PGE_2 were extracted by solid-phase extraction, and PGE_2 formation was quantified by RP-HPLC, as previously described [39].

4.3.2. Expression, purification and activity assay of human recombinant sEH

Human recombinant sEH was expressed and purified as reported before [40]. Briefly, Sf9 cells were infected with a recombinant baculovirus, provided by Dr. B. Hammock, University of California, Davis, CA. After 72 h from the transfection, cells were harvested and sonicated (3 × 10 s at 4 °C) in lysis buffer consisting of $NaHPO_4$ (50 mM, pH 8), NaCl (300 mM), glycerol (10%), EDTA (1 mM), phenylmethanesulfonyl fluoride (1 mM), leupeptin (10 μg/mL), and soybean trypsin inhibitor (60

μg/mL). Then, cells were submitted to centrifugation at 100,000×*g* (60 min, 4 °C), and the supernatants were collected and subjected to a benzylthio-sepharose-affinity chromatography. sEH was purified by elution with 4-fluorochalcone oxide in PBS containing dithiotreitol (1 mM) and EDTA (1 mM). The enzyme was then dialyzed and concentrated using Millipore Amicon-Ultra-15 centrifugal filters and wash buffer, then verifying the purity by SDS-PAGE. Finally sEH activity was determined by using a fluorescence-based assay as described before [34]. For evaluation of the test compounds, sEH was diluted in Tris buffer (25 mM, pH 7) supplemented with BSA (0.1 mg/mL) to an appropriate enzyme concentration (depending on the measured activity) and pre-incubated with test compounds or the reference compound (AUDA) or vehicle (1% DMSO) for 15 min at room temperature (rt). The reaction was started by the addition of 50 μM 3-phenyl-cyano (6-methoxy-2-naphthalenyl) methyl ester-2-oxiraneacetic acid (PHOME), a non-fluorescent compound which is enzymatically transformed into fluorescent 6-methoxy--naphtaldehyde at room temperature. The reaction was stopped after 1 h by $ZnSO_4$ (200 mM), and fluorescence was detected (λ_{em} 465 nm, λ_{ex} 330 nm).

4.3.3. Determination of COX activity

Isolated ovine COX-1 and recombinant human COX-2, respectively, were used for the determination of the activity of compounds **3**, **9**, and **21**. COXs were diluted in Tris buffer (100 mM, pH 8) supplemented with GSH (5 mM), EDTA (100 μM) and hemoglobin (5 μM) to a final concentration of 50 U/mL and 20 U/mL for COX-1 and COX-2, respectively, and pre-incubated with test compounds or the reference compound (Indomethacin) or vehicle (0.1% DMSO) for 5 min at RT. After 1 min at 37 °C, the reactions were started adding arachidonic acid to a final concentration of 5 μM for COX-1 and 2 μM for COX-2, and incubated for 5 min at 37 °C. Then, 1 mL of ice-cold methanol was added and the reactions were stopped on ice. Internal PGB_1 standard (200 ng) was added and solid phase extraction was performed as reported before [35]. COX product formation was determined by analysis of 12-HHT formation using RP-HPLC [35].

4.3.4. Cell-free 5-LO activity assay

Human recombinant 5-LO was expressed in *E.Coli* BL21 transformed with pT3-5-LO plasmid at 30 °C overnight as described before [35]. A lysis buffer was added containing triethanolamine (50 mM, pH 8.0), EDTA (5 mM), phenylmethanesulfonyl fluoride (1 mM), soybean trypsin inhibitor (60 μg/mL), dithiothreitol (2 mM) and lysozyme (1 mg/mL) and cells were homogenized by sonification (3 × 15 s). After centrifugation (40,000×*g*, 20 min, 4 °C), the supernatant was collected. The enzyme was purified using an ATP-agarose column and diluted with PBS pH 7.4 containing 1 mM EDTA. Then, 0.5 μg purified 5-LO in 1 mL PBS containing 1 mM EDTA were pre-incubated with test compounds or the reference compound (Zileuton) or vehicle (0.1% DMSO) for 10 min on ice. To start the reaction, 20 μM AA and 2 mM $CaCl_2$ were added, and the samples were incubated at 37 °C for 10 min. Ice-cold methanol (1 mL) was added to stop the reactions, and 530 μL acidified PBS and the internal PGB_1 standard were added. Solid phase extraction was performed using C18 RP-columns (100 mg, UCT, Bristol, PA, USA), and 5-LO products were quantified by RP-HPLC as previously described [35].

4.3.5. Cells

Human neutrophils and monocytes were freshly isolated from leukocyte concentrates obtained from the Institute of Transfusion Medicine, University Hospital Jena. Donors were healthy adult male and female volunteers and gave written consent, after they were informed about the aim of the study. The ethical commission of the University Hospital in Jena approved the protocol for experiments, and all methods were performed in accordance with the relevant guidelines and regulations. Briefly, neutrophils were isolated [41] by dextran sedimentation, centrifugation on lymphocyte separation medium (LSM 1077, PAA, Coelbe, Germany) and hypotonic lysis of erythrocytes. Neutrophils were resuspended in PBS pH 7.4 containing glucose (0.1%) to a final cell density of 5×10^6 cells/ml. Monocytes were separated from peripheral blood mononuclear cells (PBMC) by adherence to cell culture flasks (Greiner Bio-one, Nuertingen, Germany) for 1.5 h (37 °C, 5% CO_2) in RPMI 1640 containing L-glutamine (1 mM), heat-inactivated FCS (10%), penicillin (100 U/mL) and streptomycin (100 μg/mL), followed by cell-scraping and resuspension in PBS pH 7.4.

4.3.6. Determination of 5-LO products in intact cells

Freshly isolated neutrophils were resuspended in PBS pH 7.4 containing 0.1% glucose and 1 mM $CaCl_2$ to a final cell density of 5×10^6. Cells were pre-incubated with test compounds or Zileuton or 0.1% DMSO as vehicle for 10 min at 37 °C. For cell stimulation, 2.5 μM Ca^{2+}-ionophore A23187 (with or without supplementation of 20 μM AA) was added, and cells were kept at 37 °C for 10 min. The reaction was stopped on ice, after the addition of 1 mL ice-cold methanol. 530 μL acidified PBS and PGB_1 as internal standard were added. Afterwards, cells were centrifuged (2000×*g*, 10 min, rt) and subjected to solid phase extraction. 5-LO products formation was quantified by RP-HPLC as described above [35].

4.3.7. Analysis of acute cytotoxicity

The viability of monocytes was determined by MTT assay as described [42]. Briefly, monocytes were treated with vehicle (0.3% v/v DMSO, negative control) or test compounds and incubated for 24 h at 37 °C and 5% CO_2. MTT (Sigma-Aldrich) solution was added, cells were incubated for further 4 h, lysed in buffer containing 10% (w/v) SDS (Sigma-Aldrich), and the absorbance was measured at 570 nm (Multiskan Spectrum, Thermo Fisher, Waltham, MA).

4.3.8. Statistics

Data are expressed as mean ± S.E.M. IC_{50} values were calculated by nonlinear regression using GraphPad Prism Version 6 software (San Diego, CA) one site binding competition. Statistical evaluation of the data was performed by one-way ANOVA followed by a Bonferroni post hoc test for multiple comparison.

Declaration of competing interest

The authors declare that they have no known competing financial interests or personal relationships that could have appeared to influence the work reported in this paper.

Acknowledgements

The research leading to these results has received funding from AIRC under IG 2018 - ID. 21397 project – P.I. Bifulco Giuseppe, and funding to O.W. by the Deutsche Forschungsgemeinschaft (DFG, German Research Foundation) – project number 316213987 – SFB 1278 PolyTarget (project A04).

Appendix A. Supplementary data

Supplementary data to this article can be found online at https://doi.org/10.1016/j.ejmcr.2022.100046.

References

[1] J. Ke, Y. Yang, Q. Che, F. Jiang, H. Wang, Z. Chen, M. Zhu, H. Tong, H. Zhang, X. Yan, X. Wang, F. Wang, Y. Liu, C. Dai, X. Wan, Prostaglandin E_2 (PGE_2) promotes proliferation and invasion by enhancing SUMO-1 activity via EP4 receptor in endometrial cancer, Tumor Biol. 37 (2016) 12203–12211, https://doi.org/10.1007/2Fs13277-016-5087-x.

[2] A. Koeberle, O. Werz, Perspective of microsomal prostaglandin E_2 synthase-1 as drug target in inflammation-related disorders, Biochem. Pharmacol. 98 (2015) 1–15, https://doi.org/10.1016/j.bcp.2015.06.022.

[3] F. Bergqvist, R. Morgenstern, P.-J. Jakobsson, A review on mPGES-1 inhibitors: from preclinical studies to clinical applications, Prostaglandins Other Lipid Mediat. 147 (2020), 106383, https://doi.org/10.1016/j.prostaglandins.2019.106383.

[4] A. Koeberle, S.A. Laufer, O. Werz, Design and development of microsomal prostaglandin E_2 synthase-1 inhibitors: challenges and future directions, J. Med. Chem. 59 (2016) 5970–5986, https://doi.org/10.1021/acs.jmedchem.5b01750.

[5] C. McReynolds, S.H. Hwang, J. Yang, D. Wan, K. Wagner, C. Morisseau, D. Li, W. Schmidt, B.D. Hammock, Pharmaceutical effects of inhibiting the soluble epoxide hydrolase in canine osteoarthritis, Front. Pharmacol. 10 (2019) 533, https://doi.org/10.3389/fphar.2019.00533.

[6] Q. Qu, W. Xuan, G.H. Fan, Roles of resolvins in the resolution of acute inflammation, Cell Biol. Int. 39 (2015) 3–22, https://doi.org/10.1002/cbin.10345.

[7] A. Koeberle, O. Werz, Natural products as inhibitors of prostaglandin E(2) and pro-inflammatory 5-lipoxygenase-derived lipid mediator biosynthesis, Biotechnol. Adv. 36 (2018) 1709–1723, https://doi.org/10.1016/j.biotechadv.2018.02.010.

[8] G. Lauro, M. Manfra, S. Pedatella, K. Fischer, V. Cantone, S. Terracciano, A. Bertamino, C. Ostacolo, I. Gomez-Monterrey, M. De Nisco, R. Riccio, E. Novellino, O. Werz, P. Campiglia, G. Bifulco, Identification of novel microsomal prostaglandin E_2 synthase-1 (mPGES-1) lead inhibitors from Fragment Virtual Screening, Eur. J. Med. Chem. 125 (2017) 278–287, https://doi.org/10.1016/j.ejmech.2016.09.042.

[9] G. Lauro, M. Strocchia, S. Terracciano, I. Bruno, K. Fischer, C. Pergola, O. Werz, R. Riccio, G. Bifulco, Exploration of the dihydropyrimidine scaffold for the development of new potential anti-inflammatory agents blocking prostaglandin E_2 synthase-1 enzyme (mPGES-1), Eur. J. Med. Chem. 80 (2014) 407–415, https://doi.org/10.1016/j.ejmech.2014.04.061.

[10] G. Lauro, V. Cantone, M. Potenza, K. Fischer, A. Koeberle, O. Werz, R. Riccio, G. Bifulco, Discovery of 3-hydroxy-3-pyrrolin-2-one-based mPGES-1 inhibitors using a multi-step virtual screening protocol, MedChemComm 9 (2018) 2028–2036, https://doi.org/10.1039/c8md00497h.

[11] G. Lauro, S. Terracciano, V. Cantone, D. Ruggiero, K. Fischer, S. Pace, O. Werz, I. Bruno, G. Bifulco, A combinatorial virtual screening approach driving the synthesis of 2, 4-thiazolidinedione-based molecules as new dual mPGES-1/5-LO inhibitors, ChemMedChem 15 (2020) 481–489, https://doi.org/10.1002/cmdc.201900694.

[12] M.G. Chini, A. Giordano, M. Potenza, S. Terracciano, K. Fischer, M.C. Vaccaro, E. Colarusso, I. Bruno, R. Riccio, A. Koeberle, O. Werz, G. Bifulco, Targeting mPGES-1 by a combinatorial approach: identification of the aminobenzothiazole scaffold to suppress PGE_2 levels, ACS Med. Chem. Lett. 11 (2020) 783–789, https://doi.org/10.1021/acsmedchemlett.9b00618.

[13] R. Ottana, R. Maccari, M.L. Barreca, G. Bruno, A. Rotondo, A. Rossi, G. Chiricosta, R. Di Paola, L. Sautebin, S. Cuzzocrea, M.G. Vigorita, 5-Arylidene-2-imino-4-thiazolidinones: design and synthesis of novel anti-inflammatory agents, Bioorg. Med. Chem. 13 (2005) 4243–4252, https://doi.org/10.1016/j.bmc.2005.04.058.

[14] T. Kline, H.B. Felise, K.C. Barry, S.R. Jackson, H.V. Nguyen, S.I. Miller, Substituted 2-imino-5-arylidenethiazolidin-4-one inhibitors of bacterial type III secretion, J. Med. Chem. 51 (2008) 7065–7074, https://doi.org/10.1021/2Fjm8004515.

[15] T. Sjögren, J. Nord, M. Ek, P. Johansson, G. Liu, S. Geschwindner, Crystal structure of microsomal prostaglandin E_2 synthase provides insight into diversity in the MAPEG superfamily, Proc. Natl. Acad. Sci. U.S.A. 110 (2013) 3806–3811, https://doi.org/10.1073/pnas.1218504110.

[16] M.A. Schiffler, S. Antonysamy, S.N. Bhattachar, K.M. Campanale, S. Chandrasekhar, B. Condon, P.V. Desai, M.J. Fisher, C. Groshong, A. Harvey, M.J. Hickey, N.E. Hughes, S.A. Jones, E.J. Kim, S.L. Kuklish, J.G. Luz, B.H. Norman, R.E. Rathmell, J.R. Rizzo, T.W. Seng, S.J. Thibodeaux, T.A. Woods, J.S. York, X.-P. Yu, Discovery and characterization of 2-acylaminoimidazole microsomal prostaglandin E synthase-1 inhibitors, J. Med. Chem. 59 (2016) 194–205, https://doi.org/10.1021/acs.jmedchem.5b01249.

[17] D. Li, N. Howe, A. Dukkipati, S.T.A. Shah, B.D. Bax, C. Edge, A. Bridges, P. Hardwicke, O.M.P. Singh, G. Giblin, A. Pautsch, R. Pfau, G. Schnapp, M. Wang, V. Olieric, M. Caffrey, Crystallizing membrane proteins in the lipidic mesophase. Experience with human prostaglandin E_2 synthase 1 and an evolving strategy, Cryst. Growth Des. 14 (2014) 2034–2047, https://doi.org/10.1021/2Fcg500157x.

[18] A. Daina, O. Michielin, V. Zoete, SwissADME: a free web tool to evaluate pharmacokinetics, drug-likeness and medicinal chemistry friendliness of small molecules, Sci. Rep. 7 (2017) 42717.

[19] B.A. De Marco, B.S. Rechelo, E.G. Totoli, A.C. Kogawa, H.R.N. Salgado, Evolution of green chemistry and its multidimensional impacts: a review, Saudi Pharm. J. 27 (2019) 1–8, https://doi.org/10.1016/j.jsps.2018.07.011.

[20] A.R. Surrey, The preparation of 4-thiazolidones by the reaction of thioglycolic acid with Schiff bases, J. Am. Chem. Soc. 69 (1947) 2911–2912, https://doi.org/10.1021/ja01203a507.

[21] V. Kanagarajan, J. Thanusu, M. Gopalakrishnan, Three component one-pot synthesis of novel pyrimidino thiazolidin-4-ones catalyzed by activated fly ash, Green Chem. Lett. Rev. 2 (2009) 161–167, https://doi.org/10.1080/17518250903251767.

[22] A.V. Chate, A.G. Tathe, P.J. Nagtilak, S.M. Sangle, C.H. Gill, Efficient approach to thiazolidinones via a one-pot three-component reaction involving 2-amino-1-phenylethanone hydrochloride, aldehyde and mercaptoacetic acid, Chin. J. Catal. 37 (2016) 1997–2002, https://doi.org/10.1016/S1872-2067(16)62536-6.

[23] E. Ruijter, R. Scheffelaar, R.V.A. Orru, Multicomponent reaction design in the quest for molecular complexity and diversity, Angew. Chem. Int. Ed. 50 (2011) 6234–6246, https://doi.org/10.1002/anie.201006515.

[24] A. Bolognese, G. Correale, M. Manfra, A. Lavecchia, E. Novellino, V. Barone, Thiazolidin-4-one formation. Mechanistic and synthetic aspects of the reaction of imines and mercaptoacetic acid under microwave and conventional heating, Org. Biomol. Chem. 2 (2004) 2809–2813, https://doi.org/10.1039/B405400H.

[25] A. Koeberle, U. Siemoneit, U. Buhring, H. Northoff, S. Laufer, W. Albrecht, O. Werz, Licofelone suppresses prostaglandin E_2 formation by interference with the inducible microsomal prostaglandin E_2 synthase-1, J. Pharmacol. Exp. Ther. 326 (2008) 975–982, https://doi.org/10.1124/jpet.108.139444.

[26] H.C. Shen, B.D. Hammock, Discovery of inhibitors of soluble epoxide hydrolase: a target with multiple potential therapeutic indications, J. Med. Chem. 55 (2012) 1789–1808, https://doi.org/10.1021/2Fjm201468j.

[27] G.A. Gomez, C. Morisseau, B.D. Hammock, D.W. Christianson, Human soluble epoxide hydrolase: structural basis of inhibition by 4-(3-cyclohexylureido)-carboxylic acids, Protein Sci. 15 (2006) 58–64, https://doi.org/10.1110/2Fps.051720206.

[28] M.A. Argiriadi, C. Morisseau, B.D. Hammock, D.W. Christianson, Detoxification of environmental mutagens and carcinogens: structure, mechanism, and evolution of liver epoxide hydrolase, Proc. Natl. Acad. Sci. U.S.A. 96 (1999), 10637.

[29] C. Morisseau, M.H. Goodrow, J.W. Newman, C.E. Wheelock, D.L. Dowdy, B.D. Hammock, Structural refinement of inhibitors of urea-based soluble epoxide hydrolases, Biochem. Pharmacol. 63 (2002) 1599–1608, https://doi.org/10.1016/s0006-2952(02)00952-8.

[30] A.L. Lazaar, L. Yang, R.L. Boardley, N.S. Goyal, J. Robertson, S.J. Baldwin, D.E. Newby, I.B. Wilkinson, R. Tal-Singer, R.J. Mayer, J. Cheriyan, Pharmacokinetics, pharmacodynamics and adverse event profile of GSK2256294, a novel soluble epoxide hydrolase inhibitor, Br. J. Clin. Pharmacol. 81 (2016) 971–979, https://doi.org/10.1111/bcp.12855.

[31] S.K. Anandan, H.K. Webb, D. Chen, Y.X. Wang, B.R. Aavula, S. Cases, Y. Cheng, Z.N. Do, U. Mehra, V. Tran, J. Vincelette, J. Waszczuk, K. White, K.R. Wong, L.N. Zhang, P.D. Jones, B.D. Hammock, D.V. Patel, R. Whitcomb, D.E. MacIntyre, J. Sabry, R. Gless, 1-(1-acetyl-piperidin-4-yl)-3-adamantan-1-yl-urea (AR9281) as a potent, selective, and orally available soluble epoxide hydrolase inhibitor with efficacy in rodent models of hypertension and dysglycemia, Bioorg. Med. Chem. Lett. 21 (2011) 983–988, https://doi.org/10.1016/j.bmcl.2010.12.042.

[32] B.D. Hammock, C.B. McReynolds, K. Wagner, A. Buckpitt, I. Cortes-Puch, G. Croston, K.S.S. Lee, J. Yang, W.K. Schmidt, S.H. Hwang, Movement to the clinic of soluble epoxide hydrolase inhibitor EC5026 as an analgesic for neuropathic pain and for use as a nonaddictive opioid alternative, J. Med. Chem. 64 (2021) 1856–1872, https://doi.org/10.1021/acs.jmedchem.0c01886.

[33] J. Kramer, E.J.P. Proschak, Phosphatase activity of soluble epoxide hydrolase, Prostaglandins Other Lipid Mediat. 133 (2017) 88–92, https://doi.org/10.1016/j.prostaglandins.2017.07.002.

[34] B. Schiøtt, T.C.J.J. Bruice, Reaction mechanism of soluble epoxide hydrolase: insights from molecular dynamics simulations, J. Am. Chem. Soc. 124 (2002) 14558–14570, https://doi.org/10.1021/ja021021r.

[35] U. Garscha, E. Romp, S. Pace, A. Rossi, V. Temml, D. Schuster, S. König, J. Gerstmeier, S. Liening, M. Werner, H. Atze, S. Wittmann, C. Weinigel, S. Rummler, G.K. Scriba, L. Sautebin, O. Werz, Pharmacological profile and efficiency in vivo of diflapolin, the first dual inhibitor of 5-lipoxygenase-activating protein and soluble epoxide hydrolase, Sci. Rep. 7 (2017) 9398, https://doi.org/10.1016/j.prostaglandins.2017.07.002.

[36] K.R.A. Abdellatif, M.A. Abdelgawad, H.A.H. Elshemy, S.S.R. Alsayed, Design, synthesis and biological screening of new 4-thiazolidinone derivatives with promising COX-2 selectivity, anti-inflammatory activity and gastric safety profile, Bioorg. Chem. 64 (2016) 1–12, https://doi.org/10.1016/j.bioorg.2015.11.001.

[37] CombiGlide, New York, NY, 2021.

[38] Glide, New York, NY, 2021.

[39] A. Koeberle, U. Siemoneit, U. Bühring, H. Northoff, S. Laufer, W. Albrecht, O. Werz, Licofelone suppresses prostaglandin E_2 formation by interference with the inducible microsomal prostaglandin E_2 synthase-1, J. Pharmacol. Exp. Ther. 326 (2008) 975–982, https://doi.org/10.1124/jpet.108.139444.

[40] R.N. Wixtrom, M.H. Silva, B.D. Hammock, Affinity purification of cytosolic epoxide hydrolase using derivatized epoxy-activated Sepharose gels, Anal. Biochem. 169 (1988) 71–80, https://doi.org/10.1016/0003-2697(88)90256-4.

[41] A. Boyum, Isolation of mononuclear cells and granulocytes from human blood. Isolation of monuclear cells by one centrifugation, and of granulocytes by combining centrifugation and sedimentation at 1 g, Scand. J. Clin. Lab. Invest. Suppl. 97 (1968) 77–89.

[42] L. Thomas, Z. Rao, J. Gerstmeier, M. Raasch, C. Weinigel, S. Rummler, D. Menche, R. Müller, C. Pergola, A. Mosig, O. Werz, Selective upregulation of TNFα expression in classically-activated human monocyte-derived macrophages (M1) through pharmacological interference with V-ATPase, Biochem. Pharmacol. 130 (2017) 71–82, https://doi.org/10.1016/j.bcp.2017.02.004.